The effects of Akt overexpression in normal and dystrophic skeletal muscle

An inducible transgenic mouse model

Bert Blaauw

1. Introduction

Skeletal muscle is a very dynamic tissue continuously adapting itself to functional demands. The diverse range of fiber types seen in different muscles is mainly determined by how often a muscle is called upon to perform its task, while the intensity of the performed actions determines its size.
Two important pathways in determining skeletal muscle mass are the IGF-1 and myostatin pathways. Muscle-specific expression of IGF-1 leads to an increased muscle mass, regenerative capacity and muscle strength, while not inducing significant changes in fiber types. Mice which lack myostatin, a negative regulator of muscle size, show an excessive growth of their skeletal muscles. Interestingly, these muscles show an impaired force production (Amthor et al., 2007) despite their bigger dimensions and shift towards a more glycolytic phenotype.
Akt1/PKB is a serine/threonine kinase, downstream of IGF-1/PI3K that has emerged as a critical signaling component of the anabolic pathways and is activated by various stimuli including growth factors, mechanical stimuli and insulin. Three different isoforms of Akt are found, namely Akt1, Akt2 and Akt3. Activated Akt1 phosphorylates a great range of targets stimulating protein synthesis and reducing protein breakdown, while Akt2 is the isoform which regulates various aspects of glucose uptake and muscle metabolism (see figure 1).

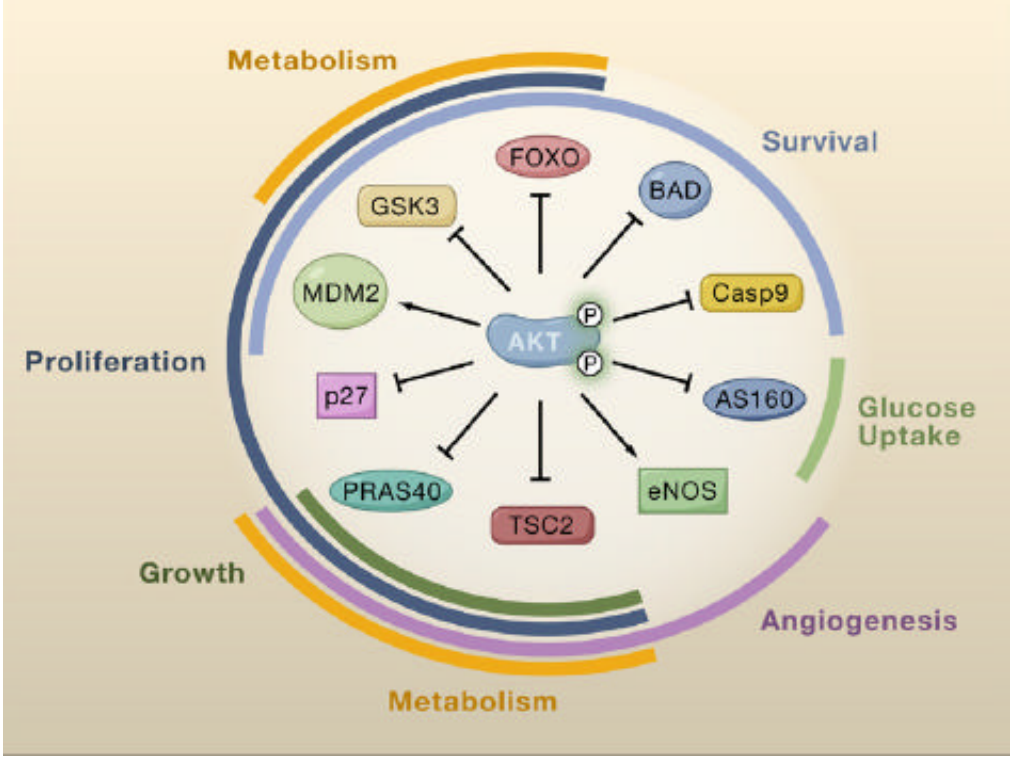

Figure 1: Akt is involved in a wide range of different cell processes

In the heart, Akt1 activation leads to an increased myocyte size. Transgenic mice over expressing a cardiac-specific constitutively active Akt1 have shown both an increased contractility and improved calcium handling. Other works sustain that activated Akt1 can lead to both a physiological as well as a pathological hypertrophy depending on the duration of Akt1 activation. Short-term activation has positive effects while long-term activation leads to contractile dysfunction and interstitial fibrosis (Schiekofer et al., 2006).
In skeletal muscles, it has been previously shown that Akt1/PKB controls muscle fibre growth in an mTOR-dependent manner (Pallafacchina et al., 2002) while simultaneously down-

modulating the activity of FoxO transcription factors, which in turn regulate the expression of two muscle-specific ubiquitin ligases, Atrogin-1 and MuRF1 (Stitt et al., 2004) (see figure 2). However, the physiological properties of muscles in which Akt activity is stimulated has not been determined. Also the conditions in which Akt is active and the mechanisms by which it is activated remain still very illusive.

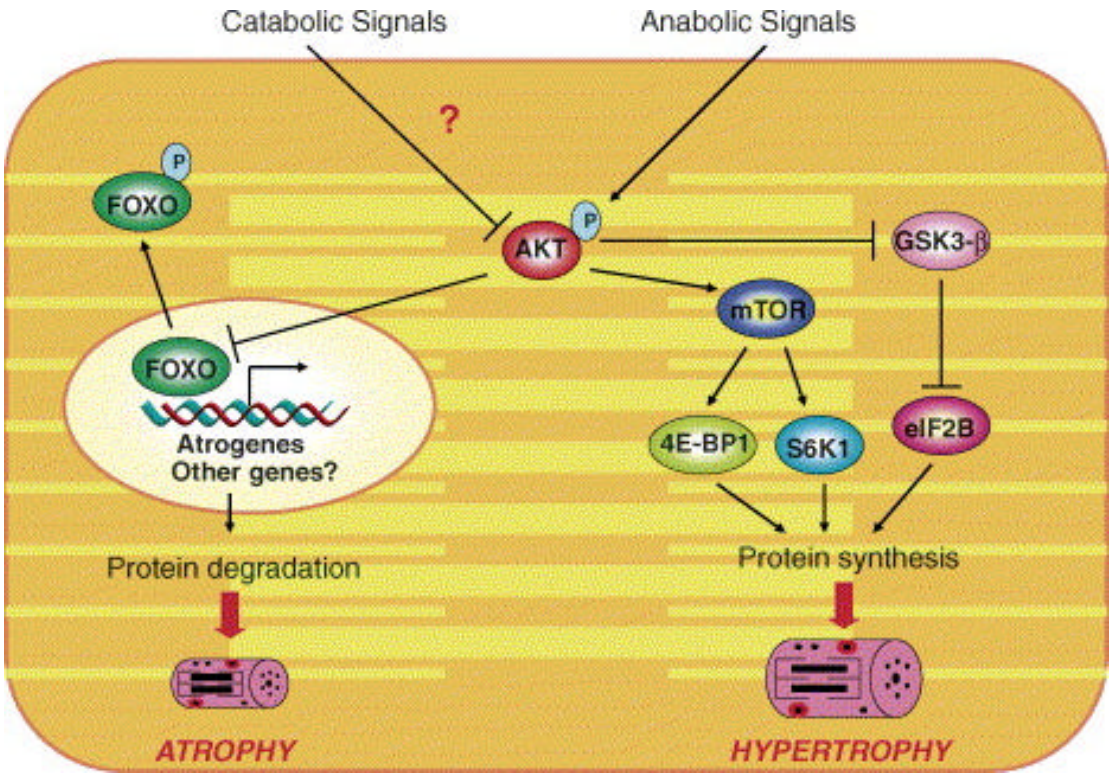

Figure 2: A schematic overview of the main pathways involved in Akt1-induced hypertrophy

In the present study we examined the effect of activation of Akt1 on skeletal muscle function. We use a wide range of techniques to fully describe the effect of Akt over-expression in normal skeletal muscle. If the hypertrophy induced by transgenically activating Akt leads to a functional hypertrophy, its therapeutic potential in Duchene muscular dystrophy is studied by crossing the transgenic mouse over-expressing Akt with the dystrophic, mdx, mouse.

In order to characterize the role of Akt in adult skeletal muscle we produced a transgenic mouse in which the expression of Akt is muscle-specific and inducible (Akt1-Cre mice). Akt activation, which was demonstrated by checking the phosphorylation status of downstream targets (i.e. FoxO3 and S6), leads to a rapidly progressing hypertrophy of all skeletal muscles. The *in vivo* model in this study was the gastrocnemius muscle, which due to its complex make-up offers insights into various aspects of muscle physiology.
The contractile performance of hypertrophic muscles was examined *in vivo* by recording gastrocnemius contractions induced by nerve stimulation under controlled loading conditions. In addition various other techniques were used to describe the effect of Akt over-expression in both healthy as well as dystrophic skeletal muscle, i.e. force measurements were performed *in vitro* on skinned fibres, electron microscopy, BrdU proliferation assays, atrophy studies, calcium transient recordings, immunohistochemistry, and general histology.

2. Materials and methods

2.1 Generation transgenic mouse model

The generation of the inducible transgenic model was achieved by crossing a transgenic line which expresses the Cre recombinase under a muscle-specific promoter (Bothe et al., 2000) with a second line which expresses Akt1 only after the deletion of an upstream DNA sequence by the Cre recombinase (Kroll et al., 2003). The myr-Akt is expressed in skeletal muscle before treatment with tamoxifen, but since it has a heat shock protein complex bound to a modified estrogen receptor domain, it cannot be phosphorylated and is therefore degraded rapidly. Akt1 phosphorylation, activation and stabilization was induced only by exogenous treatments with tamoxifen, which binds the estrogen receptor (Kroll et al., 2003).

After one injection Akt1 remains phosphorylated for approximately 48 hrs, leading us to use a protocol of injecting 1mg of tamoxifen, dissolved in ethanol and sunflower oil, once every other day. Control animals were injected only with the mix of ethanol and sunflower oil and are therefore referred to as the oil-group. Akt activation was demonstrated by checking the phosphorylation status of downstream targets, i.e. FoxO3 and S6. In most studies, mice were treated for a period of three weeks.

To study the effect of Akt overexpression in dystrophic mice, mdx (a spontaneous mutation in these mice leads to the complete absence of dystrophin in their muscles) mice were crossed with the Akt-cre transgenic mice. These mice had a mixed CD1/c57bl6-background. Indeed, the cross between the two lines leads to a bigger-sized animal with bigger forces than is normally seen in these mdx mice.

To block mTOR, mice were injected intraperitoneally once a day with 4mg/kg body weight rapamycin dissolved in physiological solution.

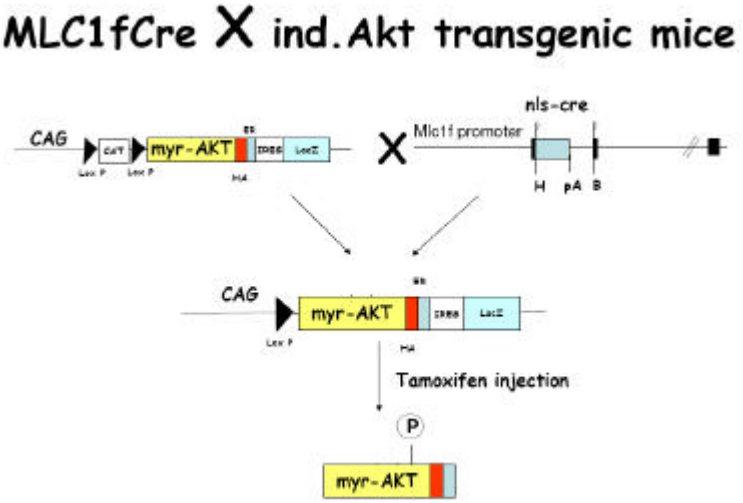

Figure 1: Crossing a muscle specific cre-line with a floxed myr-Akt leads to the inducible Akt mice used in these studies.

2.2 Denervation and spinalization

The spinalization procedure was performed under general anesthesia. The back of the mouse was shaved and disinfected with alcohol at the incision site. Skin and muscles were cut from T6 to T12 (~1 cm) with a fine scalpel, and a laminectomy was performed at the eighth thoracic vertebra. A hook was first carefully inserted beneath the exposed cord before it was surgically transected with fine scissors. To ensure completeness of the transection, the hook was then lifted through the lesion. Muscles and skin were then sutured and the mice placed in their respective cage under a heating lamp. For the whole experimental period after spinalization, manual bladder expression was performed twice daily and the hindquarters of the mice were cleaned carefully to avoid infection. Legs were moved manually to avoid

stiffness in the joints. The animals had no significant health problems except for an initial loss of body weight.
The denervation procedure was performed under general anesthesia. The mice were operated one week after the start of treatment. The treatment of the mice with either oil or tamoxifen had a total duration of three weeks. A small incision was made on the hip and the sciatic nerve was exposed and cut. Denervation was performed only on one leg, while the other served as the control. Since two weeks of denervation leads to degeneration of the distal part of the sciatic nerve, muscle stimulation was performed placing the electrodes directly on the gastrocnemius muscle.

2.3 Creatine kinase assay and Blue Evans injections
To evaluate the amount of creatine kinase present in the blood, samples of plasma were obtained using peri-orbital bleeding. By placing a piece of glass pipette of a small diameter behind the eye of the mouse and twisting gently till rupture of the vessel, around 100µl of blood was collected in a tube containing 2µl of 0,5M EDTA as anticoagulant. Creatine kinase content was measured by the accumulation of β-NADP using a kit from Sentinel Diagnostics.
As a measure for membrane permeability, the vital dye Blue Evans was used. Mice were injected i.p. with a solution containing 2% Evans Blue dye in phosphate-buffered saline (PBS, pH 7.5), with the injection volume being 0.5% relative to body mass. Muscles were examined on average one hour after cessation of stimulation. Also more extended time points were used, without any visible changes in the results.

2.4 Histology
Muscle structure was examined with Hematoxylin and Eosin staining. Cryostat sections are fixed in PFA 4% before being placed in Harris Hematoxylin, followed by a short dip in alcoholic acid and 1 minute incubation in Eosin. Hematoxylin colors the acid regions (nuclei), while Eosin colors the basic regions (cytoplasm). In fluorescence, nuclei were stained with DAPI.
Glycogen staining was done using by a periodic acid-Schiff stain. Muscles were frozen in liquid nitrogen and cryosections of 8µm were fixed in Carnoy's fixative placed in periodic acid before being transferred into Schiff's solution. This method visualizes glycogen, lipids and polysaccharides.

2.5 Electron microscopy
The small muscle specimens were fixed in 2.5% glutaraldheyde in cacodylate buffer 0.1M, post-fixed in 1% osmium tetroxide in the same buffer, dehydrated in ethanol and embedded in Araldite. Thin sections, stained with uranyl acetate and lead citrate were observed under a transmission electron microscope Philips 410.

2.6 Electrophoresis
Muscle samples for protein electrophoresis were solubilized in Laemmli solution (Tris 62.5 mM pH6.8, Glycerol 10%, SDS 2.3%, β-mercaptoethanol 5%) with E-64 0.1% and Leupeptin 0.1% (SIGMA) as antiproteolytic factors. Samples were analyzed on 8% polyacrylamide slab gels after denaturation in SDS (SDS-PAGE) with a procedure derived from Blough et.al (Blough et al., 1996), modifying stacking gel composition with glycerol 29%. Slabs 18 cm wide, 16 cm high and 1 mm thick were used. Electrophoresis was run for 46 h, at 100 V for 3 h and 230 V for the remaining time at 4°C. Gels were silver stained (Bio-Rad Silver stain plus). Four bands were separated in the region of 200 kD, corresponding, in order of migration rate from the fastest to the slowest, to MHC-1, MHC-2B, MHC-2X and MHC-2A.

2.7 Western blotting and immunohistochemistry

Antibodies used for immuno histochemistry were: mouse anti-smooth muscle actin (1:200; Sigma), mouse anti-BrdU (1:5; Roche), rabbit anti laminin (1:200; Sigma), rabbit anti-Phospho-Akt1 (1:50; Cell Signaling). Antibodies used for Western blot were rabbit anti-Akt total, rabbit anti P-S6, rabbit anti P-Akt1 ser 473, rabbit anti pan-actin (all 1:1000; Cell Signaling), mouse anti utrophin (1:50 Iowa Hybrid bank), mouse anti desmin (1:1000 Sigma), mouse anti MyHcA (Schiaffino).

FITC-, Cy3-, and Cy2-conjugated secondary antibodies (1:200) were obtained from Bio-Rad.

2.8 *In vivo* BrdU incorporation assay

Bromodeoxyuridine (BrdU) is a synthetic thymidine analog that gets incorporated into a cell's DNA when the cell is dividing (during the S-phase of the cell cycle). In order to evaluate incorporation of new nuclei into mature fibers during hypertrophy mice were injected intraperitoneally for different time periods. Every injection contained 50mg/kg BrdU dissolved in physiological solution. Total volume injected was 100µl. To identify positive nuclei, a specific staining protocol was used in which very thin cryostat sections were cut (4-6µm) and sections were incubated with both 4M HCl and trypsin, exposing the DNA to the antibody (as a consequence dapi-staining doesn't give any signal anymore).

2.9 *In vivo* muscle mechanics

Gastrocnemius muscle contractile performance was evaluated *in vivo* using a 305B muscle lever system (Aurora Scientific Inc.). In order to measure torque production the foot was fixed to a footplate, which was fixed to the shaft of the motor. Extreme care was taken to align the ankle with the axis of the motor in order to make the error in determining the lever arm as small as possible. The lever arm was determined as the distance from the ankle to the heel, 2,1mm in both hypertrophic as well as control groups. Using this lever arm we calculated force by dividing the torque by the lever. Increasing the force offset above the isometric tetanic plateau, isometric forces can be registered by connecting the motor through an A/D-converter to the computer. By using specially developed Lab View software force transients could be recorded and analyzed. To correctly evaluate force production and reduce noise in the signal, the knee was firmly fixed by two stainless steel screws as the mouse was laying face-up.

In order to elicit a contraction the tibial nerve was stimulated electrically. At the beginning of the experiment mice were anaesthetized by a mixture of Xylor and Zoletil. Once responsiveness was completely absent a small incision was made from the knee to the hip, exposing the sciatic nerve. Before the branching of the sciatic nerve, Teflon-coated 7 multistranded steel wires (AS 632, Cooner Sales, Chatsworth, CA, U.S.A.) were implanted with sutures on either side of the sciatic nerve. At the distal ends of two wires the insulation was removed, while the proximal ends were connected to a stimulator (Grass S88). In order to avoid recruitment of the dorsal flexor muscles, which are antagonist of gastrocnemius, and therefore significant reduction of torque, the common peroneal was cut.

The stimulation amplitude was determined increasing in steps the voltage to find first the threshold at which contractile response starts to appear and then a maximal intensity, ie. the voltage at which twitch tension no longer increased. Stimulus duration was kept constant at 1ms.

The following experimental protocols were employed:

a) force-frequency curves were determined by stepwise increasing stimulation frequency, pausing at least 30 seconds between stimuli to avoid effects due to fatigue.
b) force-velocity curves were obtained during tetanic contractions at 70Hz.
c) the fatigue protocol consisted of 30 Hz trains of 0, 3 seconds once every second.
d) Force-length curves were determined rotating the foot stepwise 1 mm (which equals 1/90*p rad)
e) eccentric contractions were analysed to study muscle damage. Muscle lengthening was achieved by moving the foot upward at a velocity of 40 mm/s while simoultaneously stimulating the gastrocnemius. The footplate was moved 200ms after initiation of stimulation with 100Hz, thus eccentric pull occurs during the isometric plateau of the tetanus. The range of movement during the pull was calculated to be 30°, clearly inside physiological limits of movement for the foot. Total duration of tetanic stimulation was limited to 600ms, assuring no sag of force. This protocol was repeated 20 times taking the decrease in the isometric force plateau as an indication for muscle damage.

2.10 *In vitro* mechanics on skinned fibres

Samples dissected from the superficial layers of the gastrocnemius were immersed in ice cold skinning solution (see below). Single fibers were manually dissected from fiber bundles under a stereomicroscope (10x magnification). At the end of the dissection, fibers were bathed for 1 h in skinning solution containing 1% Triton X-100 to ensure complete membrane solubilization. Segments of 1-2 mm length were then cut from the fibers and light aluminum clips were applied at both ends.
Skinning, relaxing, pre-activating and activating solutions utilized for mechanical experiments with single fibers were prepared as described by Bottinelli and coworkers (Bottinelli et al., 1996). Skinning solution was composed of (in mmol/L): Na2ATP, 3; magnesium acetate, 5; EGTA, 5; potassium dihydrogen phosphate, 5; potassium propionate, 150; dithiothreitol, 1. The pH of this solution was adjusted to 7,1 with KOH, while the three different bathing solutions had the following compositions: The solutions contained (in mmol/1): MgATP, 5; free Mg2+, 1; PEP, 10; sodium azide, 5; oligomycin B, 0-01; NADH, 0-8; P1,P5-di(adenosine-5') pentaphosphate, 0-2 and N,N-bis(2-hydroxyethyl)-2-aminoethanesulphonic acid (BES), 100. In addition, all solutions contained 4 mg/ml pyruvate kinase (500 U/ml, Sigma) and 0, 24 mg/ml lactic dehydrogenase (870 U/ml, Sigma). The pH was adjusted with KOH to 7, 1. Potassium propionate was added to adjust ionic strength to 200 mm. The relaxing solution contained 20 mM EGTA. Preactivating solution had a composition similar to the relaxing solution except that EGTA concentration was reduced to 0.5 mM and 25 mM creatine phosphate and 300 U/ml creatine phosphokinase were added. Activating solution was similar to the relaxing with the addition of 5 mM $CaCl_2$, 25 mM creatine phosphate and 300 U/ml creatine phosphokinase. The pH of all solution was adjusted to 7.1 at the temperature at which solutions were used (12°C). Protease inhibitors (E64 10 µM and leupeptine 40 µM) were present in all solutions.
In each fiber segment, isometric tension (Po) was measured during maximal activations at 20°C, pCa=4.8 under the conditions described in previous studies (Reggiani et al., 1997). The kinetics of tension redevelopment was measured from the time course of tension development after a fast (< 1 ms) maneuver of shortening to reduce tension to zero and fast re-lengthening back to the initial length after an interval of 30 ms. Tension redevelopment was recorded and characterized by the time required to redevelop 2/3 of isometric tension. Digitized images of each fiber were taken with a camera connected with the microscope at 360x magnification. Cross sectional area (CSA) was calculated from the average of three diameters, spaced at

equal intervals along the length of the fiber segment, assuming a circular shape. Sarcomere length was determined by counting sarcomeres in several intervals of 30 µm.
To study damage induced by eccentric contraction the following protocol was adopted: in each fibre segment, isometric tension (Po) was repeatedly measured during maximal activations at 20°C, pCa=4.8 under the conditions described. Two eccentric contractions were done by stretching the fibre segment 0.15 L/s for 0.7s while being activated maximally. The again maximal contractions were induced in isometric conditions. To determine the damage to the fibre, isometric tension after the two stretches was expressed in relation to isometric tension before the two stretches.

2.11 Intracellular Ca^{2+} measurements in single intact muscle fibres

Single FDB (Flexor digitorum brevis) fibers were isolated with a modified collagenase/protease method as described previously. There was no difference in fiber yield between wild type and transgenic mice. On the day of the experiment (generally 48 hours after dissociation) isolated fibers were loaded with 5µM fura-2 acetoxymethyl ester (Molecular Probes, Invitrogen) in incubation buffer (125mM NaCl, 5mM KCl, 1mM $MgSO_4$, 1mM KH_2PO_4, 5.5mM glucose, 1mM $CaCl_2$, 20mM Hepes and 1% bovine serum albumin, pH 7.4 with NaOH) for 30 min at 37°C. After loading with Fura-2, fibers were washed twice for 10 minutes with incubation buffer without BSA at 37°C to retain the indicator in the cytosol. After a minimum of 30 minutes calcium signals were recorded using a dual-beam excitation fluorescence photometry setup (IonOptix Corp.) at the temperature of 25°C. After 5–10 minutes of steady-state pacing at 0, 5 Hz, 10 transients were recorded from each fiber which was then removed with a micropipette and transferred to an Eppendorf test tube containing Laemmli solution for CS isoform identification. About five fibers were analyzed from each Petri dish. Ca^{2+} transients were analyzed using the software IonWizard designed by IonOptixCorp. $[Ca^{2+}]_i$ measurements were expressed as fluorescence ratio (F ratio), with reference to the excitation wavelengths of 360 and 380 nm used to monitor the fluorescence signals of Ca^{2+}-bound and Ca^{2+}-free fura-2, respectively.

3.1 Effects of Akt-activation in normal skeletal muscle

3.1.1 Akt induces muscle hypertrophy

Skeletal muscle specific expression of Akt1 was achieved by placing the transcription of a constitutively active Akt1 bound to an estrogen receptor under the control of a myosin light chain 1f-promoter. After injection of tamoxifen, which removes the heat shock protein complex bound to the estrogen receptor by binding to the estrogen receptor itself, Akt1 is rapidly phosphorylated and can phosphorylate its downstream targets. One single intraperitoneal injection (1,5mg per animal) is sufficient to keep Akt1 phosphorylated for about 48hrs. Injecting tamoxifen for one week is sufficient to induce a large hypertrophy which is limited to skeletal muscle (no cardiac hypertrophy seen, unpublished observations) there is no leakage of the transgenic system as vehicle (oil)-treated animals showed no hypertrophy (figure 1).

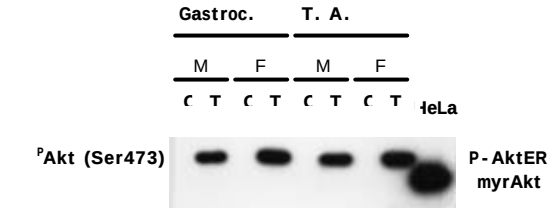

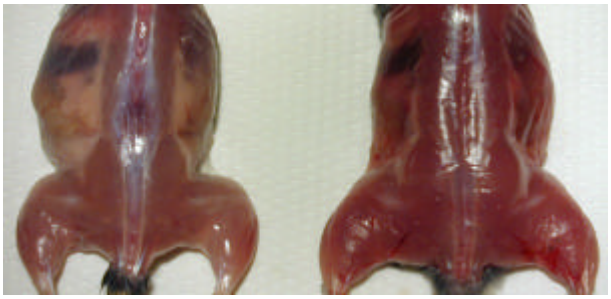

Figure 1: The western blot (left panel) shows the clear posphorylation of Akt after injection of tamoxifen and not when injecting the vehicle. The results of three weeks of activation are clearly seen in the right panel. Also note the reduction in fat white strips.

Muscle hypertrophy was present in both male and female mice and was seen in all muscles studied, even though some muscles responded with a bigger increase in wet weight than others. This differential response to Akt1 activation was not due to an inhomogeneous expression of the transgene as all fibers from each muscle showed a clear activation of Akt1, regardless their type (slow or fast), see figure 2.

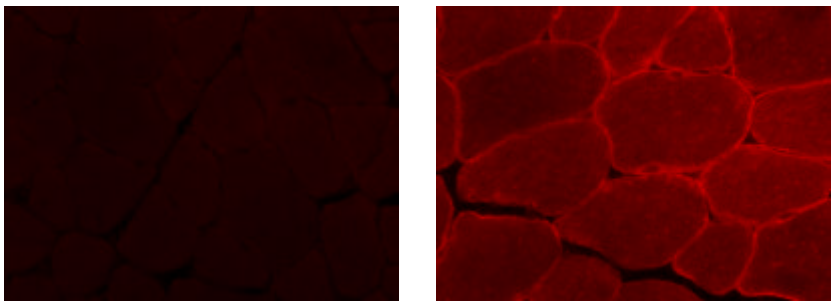

oil **tam**

Figure 2: Immuno-histo chemistry for P-Akt, clearly showing a membrane staining with also a diffuse cytoplasmatic coloration present in all fibers.

The muscle selected for physiological evaluation was the gastrocnemius due to its complex make-up and substantial hypertrophic response to akt activation after three weeks of tamoxifen treatment. The most substantial growth occurs during the first week of treatment after which muscle weight seems to slowly level off (table 1).

	Females 1 week	**Females 3 weeks**	**Males 1 week**	**Males 3 weeks**
Weight oil (mg)	**161 ± 4**	**156 ± 4**	**190 ± 6**	**176 ± 7**
Weight tam (mg)	**224 ± 6**	**239 ± 6**	**246 ± 3**	**261 ± 4**

Table 1: Gastrocnemius weights after 1 week (every day injection) compared to three weeks (every other day injection) of treatment.

When comparing the hypertrophic response in both the oxidative, deep and the glycolytic, superficial part of the gastrocnemius the response to akt activation, it seems plausible to assume that akt induces hypertrophy independent of fiber-type (figure 3). Supporting this statement is that the relative increase in wet weight in the soleus is comparable to that seen in the EDL (our observations).

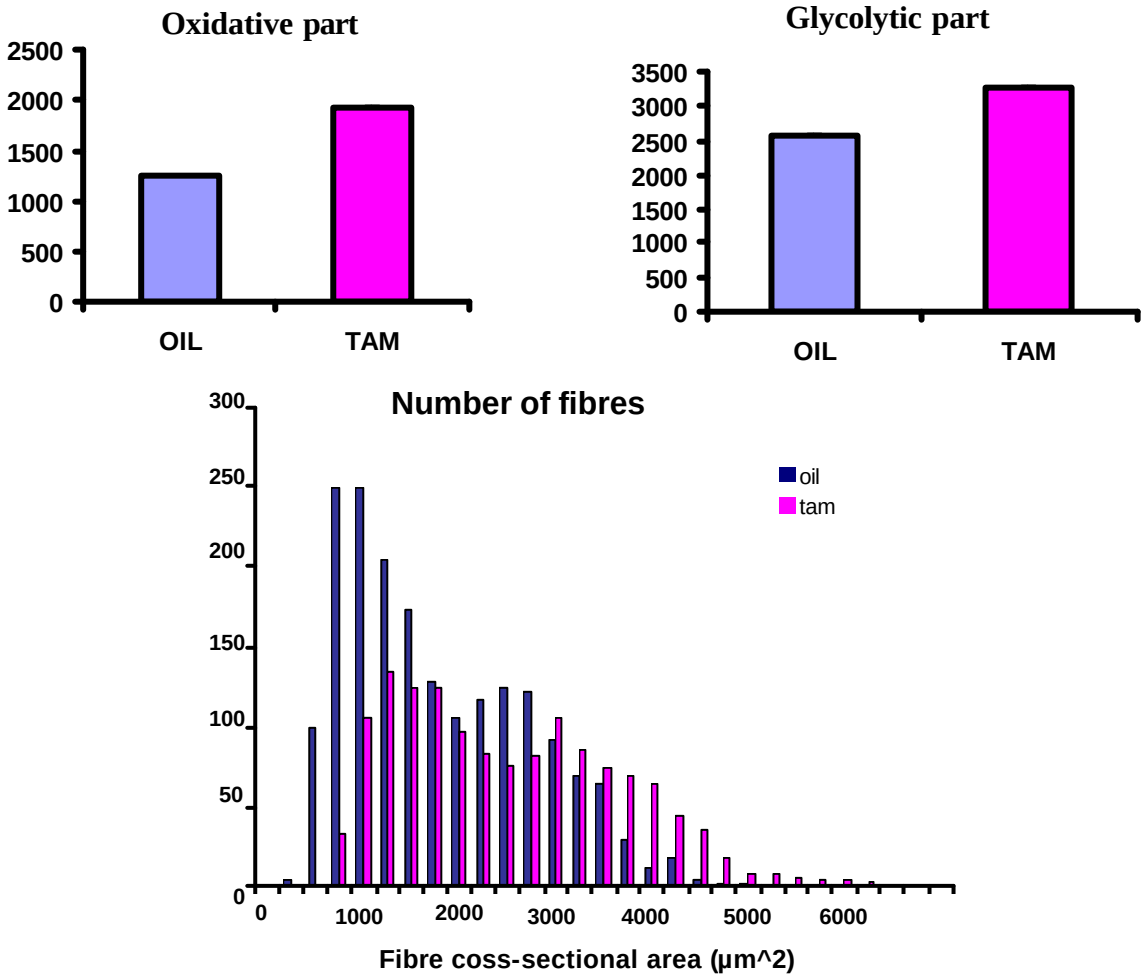

Figure 3: Akt increases muscle size independent of muscle fiber type, as can be seen by measuring the average cross-sectional area of hypertrophic fibres (after 3 weeks) for both the internal oxidative part as well as the glycolytic external part. The last graph shows the overall increase in single fiber area.

3.1.2 Akt increases muscle strength *in vivo*

To assess whether a proportional increase in contractile strength accompanied Akt-induced hypertrophy, we set up a system which enables us to measure torque transients of the hindleg *in vivo*. Maximal muscle activation was obtained by supramaximally stimulating the tibial nerve while the torque was measured by keeping the foot fixed on a footplate. Muscle force was calculated by dividing the produced torque by the lever, i.e. the distance between the tendon attachment and the ankle pivot. Motor axis and ankle pivot were carefully aligned for every experiment.

After three weeks of Akt activation there was a clear increase in absolute force production in both males and females (figure 4). Hypertrophic animals showed a 15% and 53% increase in twitch force for respectively males and females. Maximum force was obtained when stimulating at 100Hz and this tetanic force was also 15% and 26% higher in hypertrophic compared to control animals, for respectively males and females.

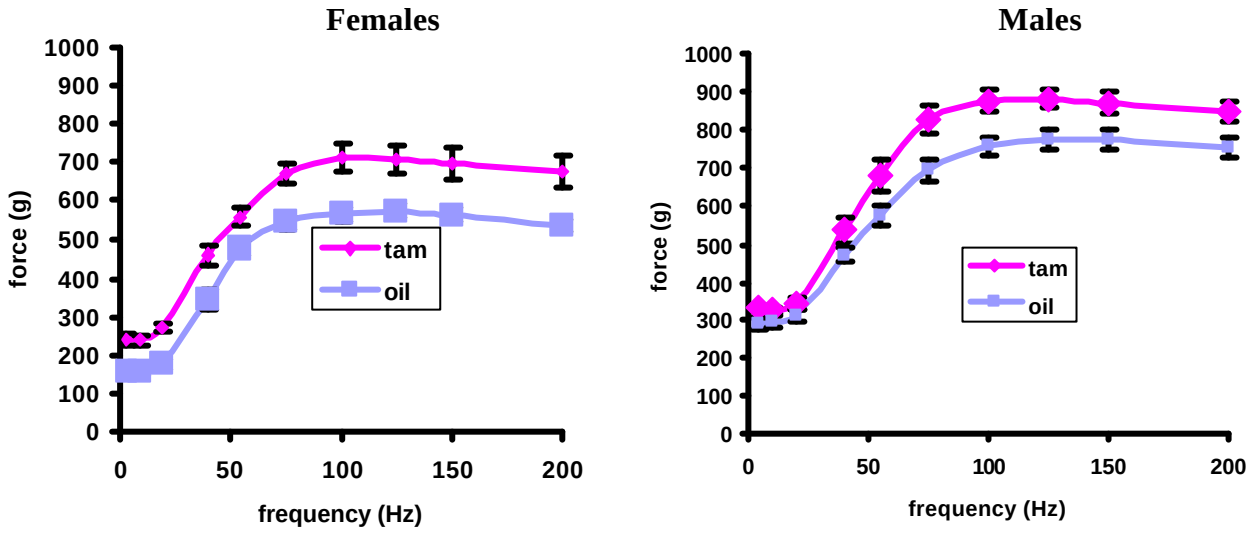

Figure 4: Absolute force after three weeks of akt-phosphorylation (tam) and in control animals (oil). Both males and females show a significant increase in absolute force.

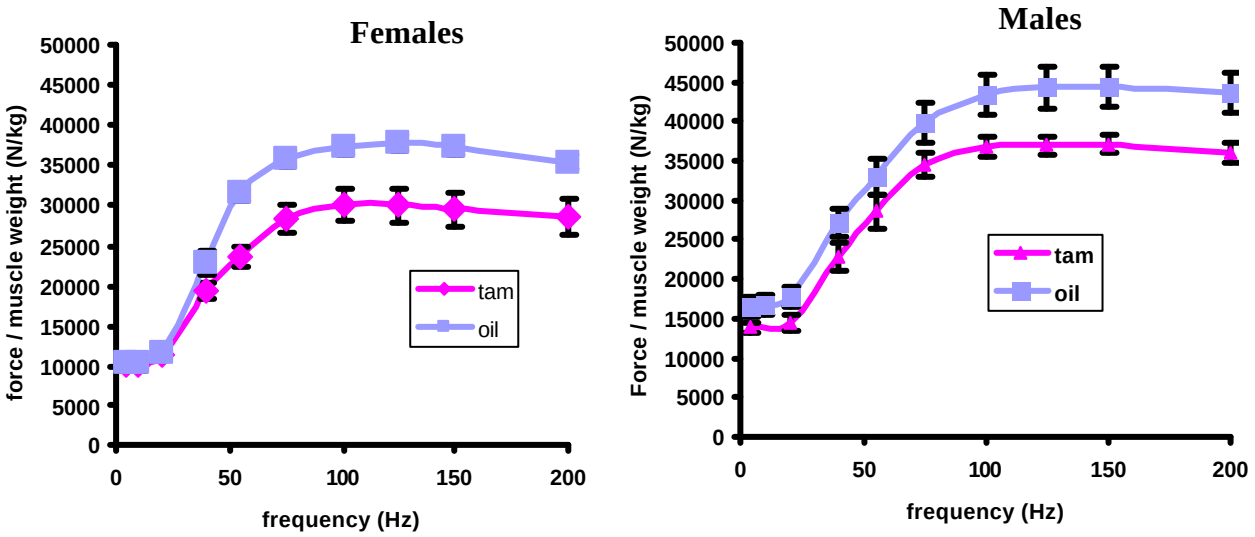

Figure 5: Force normalized for muscle mass. As can be seen clearly, normalized force is lower in hypertrophic animals compared to controls for both males and females.

When normalizing force for muscle weight, in agreement with the observation that the muscle weight increased by 48% in males and 53% in females, it was clear that the increase in force was not proportional to the increase in muscle weight.
An additional surprising observation was that force increased already after one week of activation in females, while males only show an increase after three weeks of activation (data not shown).
When evaluating twitch times, hypertrophic animals consistently showed a slight, but significant increase in time to peak and half relaxation time (figure 6).
To evaluate metabolic performance of these hypertrophic muscles, a low frequency fatigue protocol was used. The relative force decrease after 400 seconds of fatiguing electrical stimulation did not show any difference between control and tam-treated animals (figure 7).

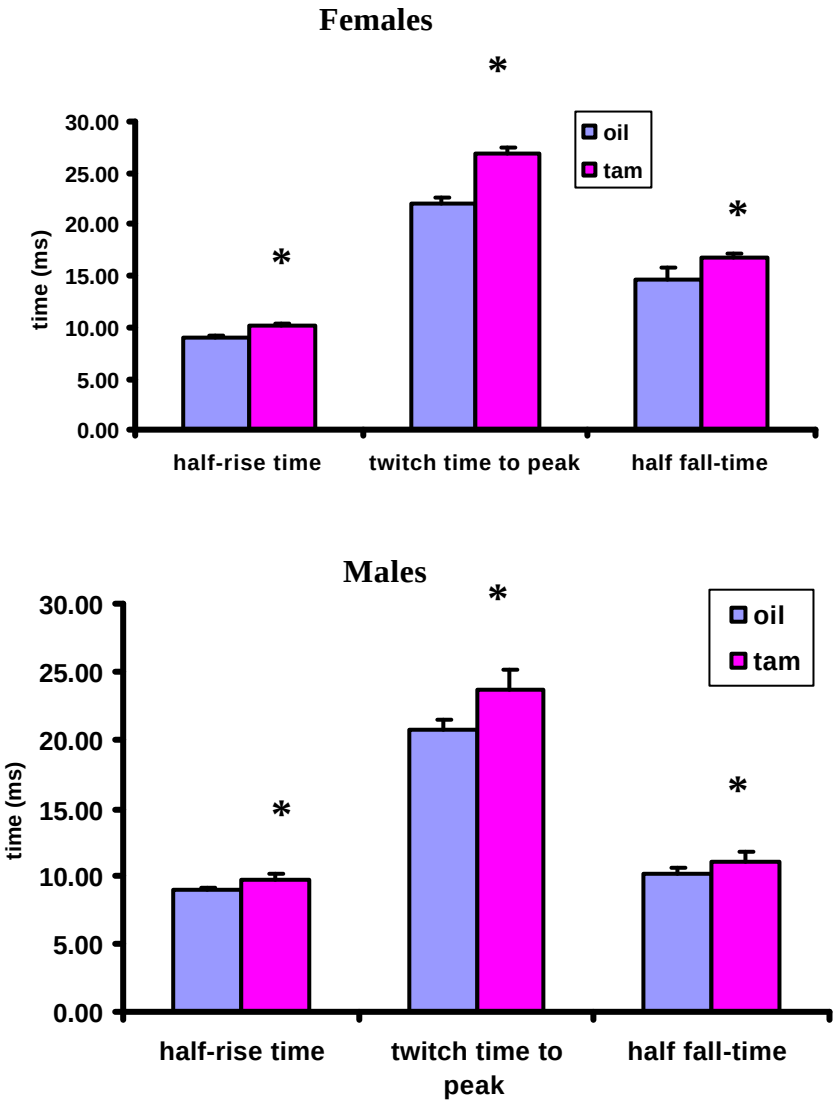

Figure 6: Twitch time parameters are slower in hypertrophic animals.

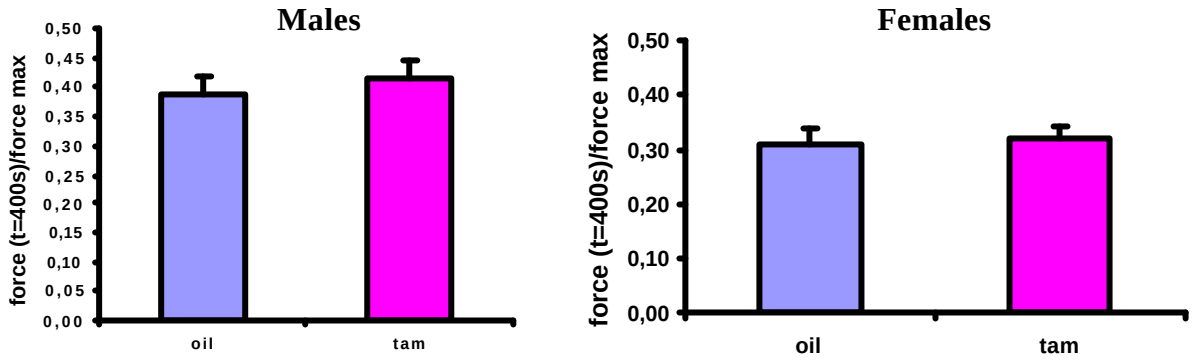

Figure 7: Residual force after 400 seconds of fatiguing stimulation protocol at a duty cycle of 0, 3 indicates a similar force reduction in both hypertrophic and controls.

3.1.3 Akt increases calcium release in single fibers

In order to ascertain that an increase in dimensions is followed by an increased calcium release we performed measurements of the calcium transients in isolated single fibers from the flexor digitorum brevis (FDB). A few days after plating, cells were loaded with Fura-2 and stimulated electrically. Using this ratiometric approach we showed a clear increase in peak transient in hypertrophic fibers when electrically stimulated with low frequency (twitches) (figure 3c). This 20% increase in peak transient implies an increased calcium release. Transient time parameters were unchanged despite the higher peak value, likely indicating an increased release- and re-uptake velocity.

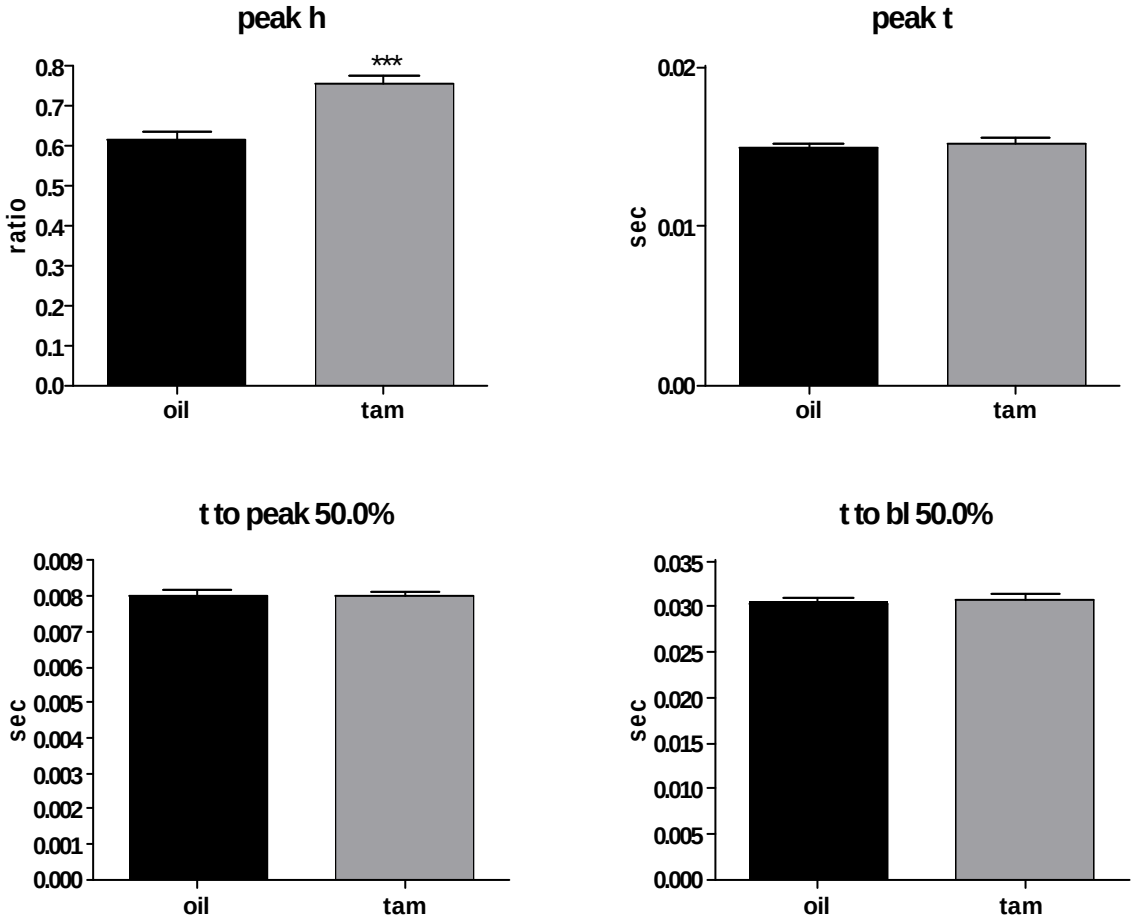

Figure 11: Calcium transients in single fibers from the FDB after electrical stimulation show an increased amplitude in hypertrophic fibers (top left panel). Transient kinetics however have not changed as is seen by similar transient times (lower two and top right panel).

3.1.4 Strength in skinned fibers from hypertrophic muscles increases

To assess whether the decrease in normalized force was due to a defective actin-myosin interaction we examined force production in skinned single fibers taken from the external, glycolytic, part of the gastrocnemius. To measure the force produced single fibers are dissected, permeabilized with Triton and placed on the set-up for recording mechanical parameters. Before initiating force measurements the diameter was determined, showing an 23% increase in hypertrophic animals compared to vehicle treated animals (figure 8).

Figure 8: Cross-sectional area of skinned fibers. When comparing this graph with the glycolytic fiber cross sectional area from figure 3 it is clear that oil fibers swell more than hypertrophic fibers.

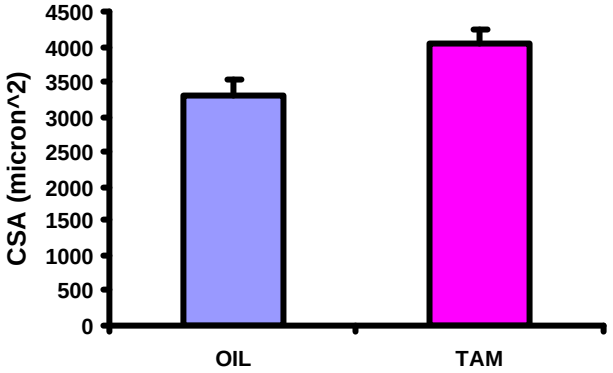

Surprisingly, this increase in diameter was significantly smaller than the 38% increase observed in the glycolytic part of the controlateral legs of both tamoxifen and oil-treated animals when determined in cryostat cross-sections. In order to analyze the discrepancy we calculated the amount of swelling as determined by dividing the average fiber cross sectional area in the skinned fibers preparation by the average fiber cross sectional area as found in cryostat cross-sections from the controlateral leg in control and hypertrophic animals. The increase in cross sectional area due to swelling was in control animals of 25% as compared to an increase of 11% in hypertrophic fibers, suggesting a more rigid cytoskeleton in hypertrophic fibres.

Placing these skinned fibers in a solution containing a suitable free calcium concentration to elicit a maximum contraction we observed that hypertrophic fibers developed a greater absolute force compared to vehicle treated animals (figure 9). The increase in absolute force (+98%) was reduced but not disappeared when tension was calculated by dividing force by cross sectional area. Thus it indicates that either increased density or an improved efficiency of actin-myosin interactions occurred after 3 weeks of tamoxifen administration.

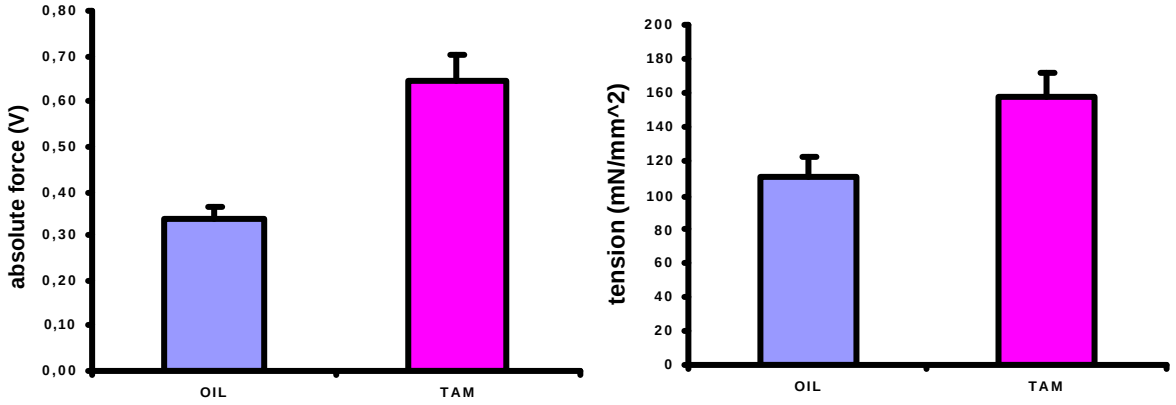

Figure 9: *The clear increase in absolute force in TAM treated animals is not completely explained by an increased diameter, as also the tension is increased*

When the fiber is quickly shortened by a very rapid movement of the lever, all actin-myosin interactions are broken and the kinetics of tension redevelopment is a direct indication of the formation of new interaction. The half-time of tension redevelopment showed a small, yet significant increase in hypertrophic animals suggesting a change in actin myosin interaction kinetics (Figure 10).

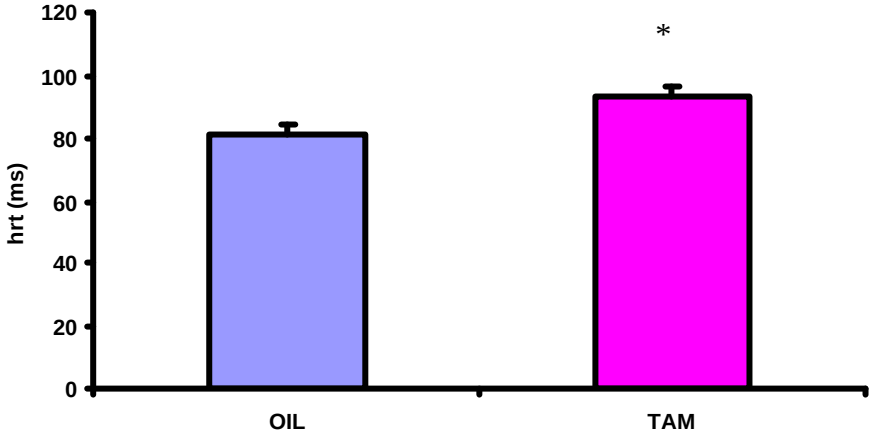

Figure 10: *Force redevelopment after a slack test in the tam-group is significantly slower compared to the oil group.*

3.5 Akt does not induce a change in myosin isoform composition

Using gel electrophoresis to separate the various myosin heavy chain-isoforms no visible difference between tamoxifen and oil treated animals was noted (figure 12). These results were confirmed by staining of cryostat cross-sections with antibodies for the different myosin heavy chain-isoforms, an example of which is given in figure 13.

Figure 12: An electrophoresis gel, revealing myosin content using silver staining, showing different myosin-isoform contents after three weeks of tam-treatment and in control muscles.

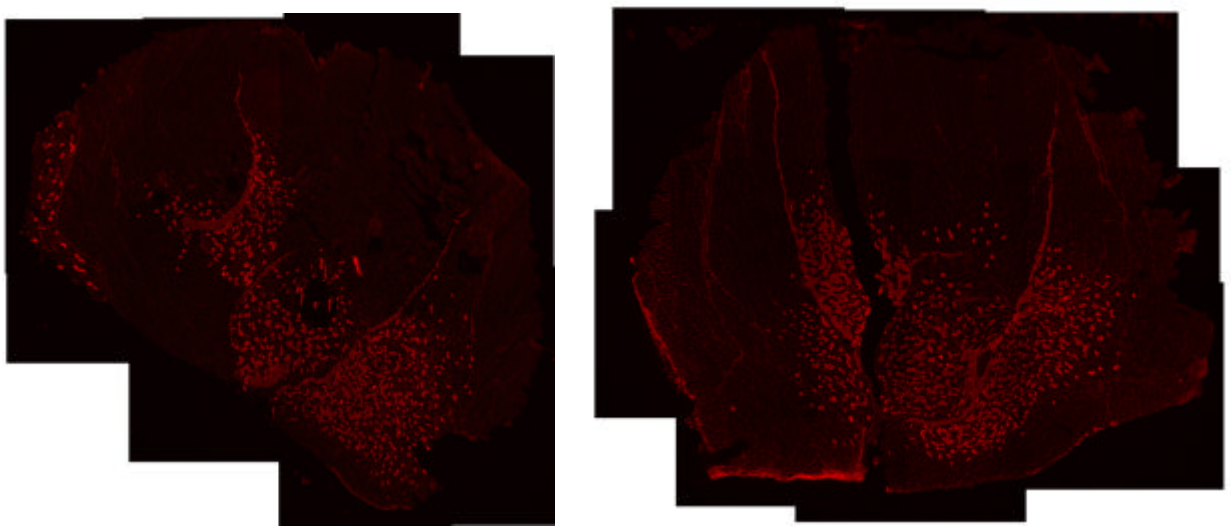

Oil (Gastrocnemius) **Tam(Gastrocnemius)**

Figure 13: No significant difference in the number of positive fibers between treated and control animals is seen after staining with the monoclonal antibody SC-71, staining for MyHC2A.

3.1.6 Akt-induced hypertrophy shows a transient glycogen accumulation

To analyze the ultra structural organization of a hypertrophic muscle, we prepared 1 week treated EDL muscles for examination by electron microscope. Analysis revealed enlarged spaces between individual myofibrils in hypertrophic animals (figure 14). Large, irregularly sized spaces between myofibrils as seen in many fibers treated with tamoxifen for one week did not appear at all in oil treated animals. Also the presence of droplets of fat was only seen in hypertrophic muscle, indicating an increased energy uptake likely in order to sustain the more demanding protein synthesis. The major source of energy for skeletal muscle is the storage of glucose in the form of glycogen inside the fiber membrane. In order to ascertain that there was indeed an increased energy storage we performed a staining for glycogen using a periodic acid Schiff staining. We found that all muscles, both males and females, showed a strong increase in glycogen content (figure 15).

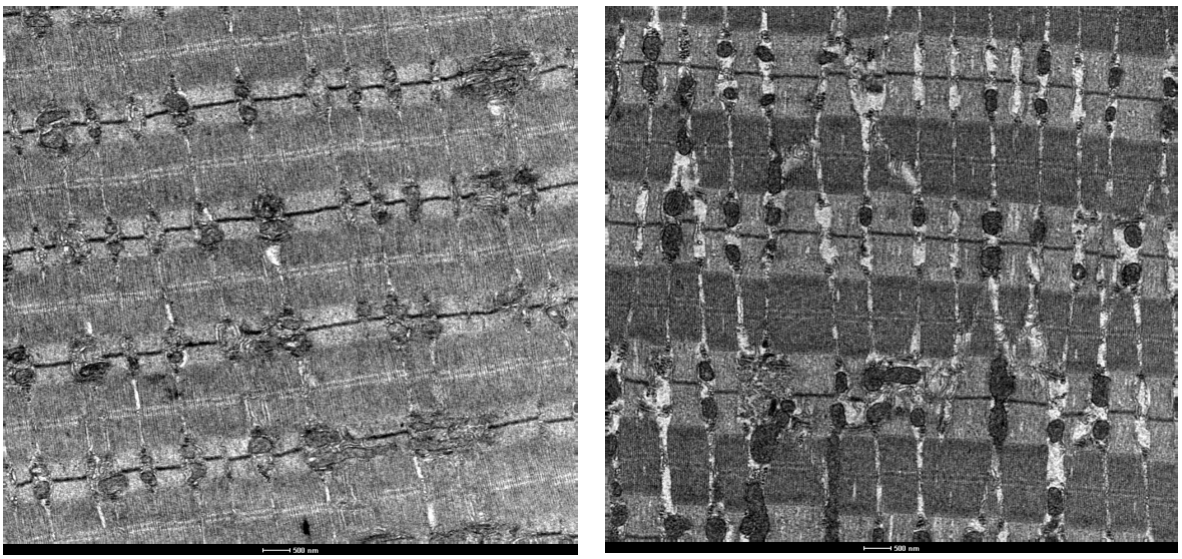

Oil **Tam**

Figure 14: Myofibrillar organization in EDL control-and hypertrophic muscles after one week of tamoxifen injections. As can clearly be seen, hypertrophic muscles don't display the normally found highly regular myofibrillar organization

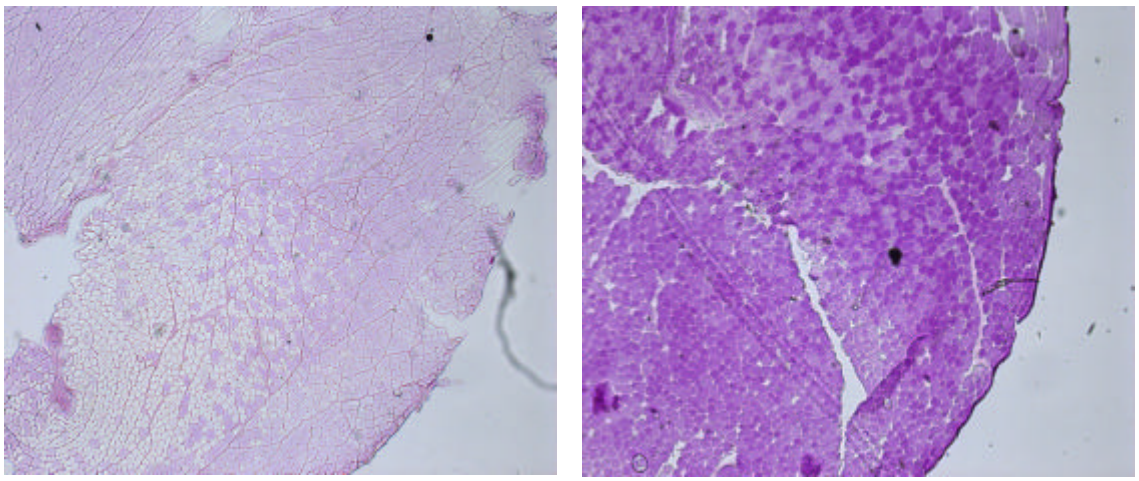

Oil **Tam**

Figure 15: PAS staining is increased in hypertrophic muscles indicating an increased glycogen content.

After three weeks of treatment with tamoxifen, electron microscope images revealed a perfect ultra structurally organization (figure 16). No more empty spaces or fat droplets were found, indicating a new steady state. Confirmation of these findings came from glycogen staining performed on 3 weeks treated muscles, showing no difference between tamoxifen treated and control muscles (figure 17). Again, all muscles, both male and female, showed this transient increase in glycogen at one week, followed by return to baseline values at three weeks of treatment. This transient increase in glycogen content was seen in both slow and fast muscle fiber types.

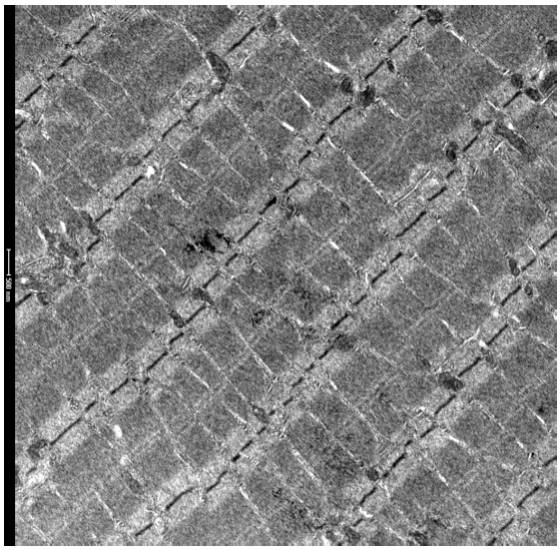

Oil

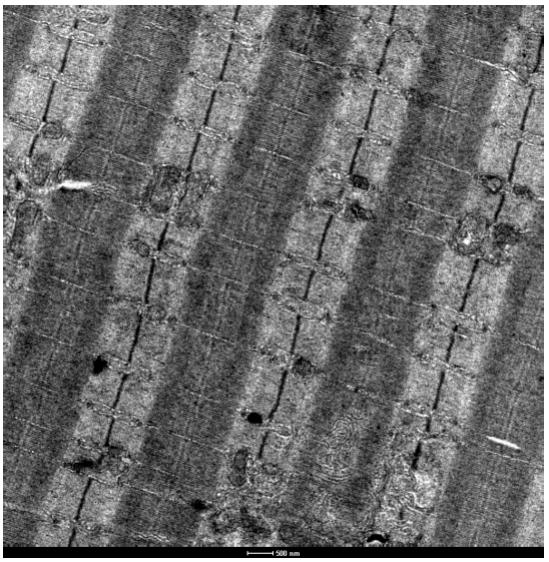

Tam

Figure 16: After three weeks of treatment hypertrophic muscles show an ultra structure similar to controls

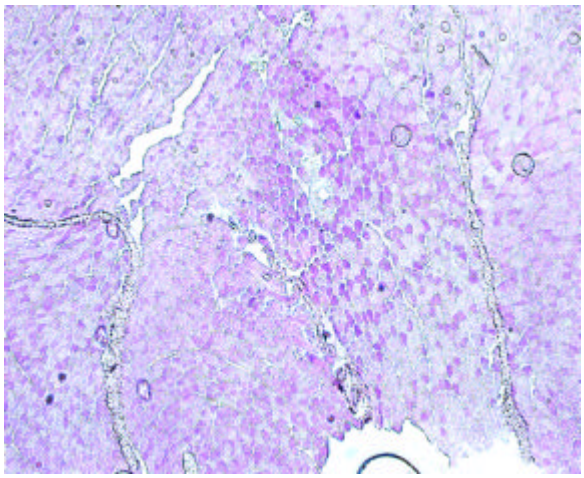

Oil (Gastrocnemius)

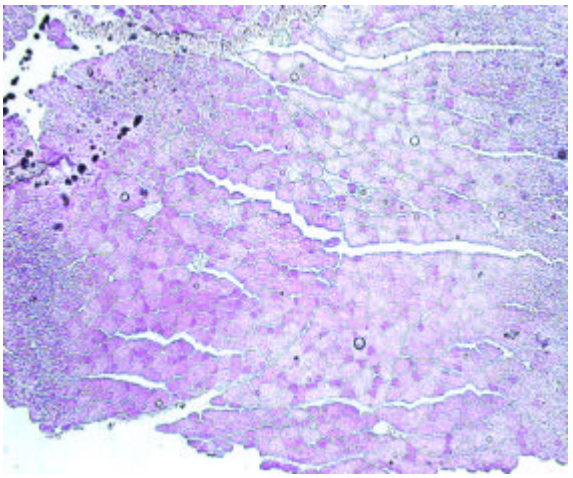

Tam (Gastrocnemius)

Figure 17: After three weeks of treatment glycogen content returns to baseline levels.

A further support to the view of a transient change in metabolic conditions came from micro-array data which were taken from both tam and oil treated animals at various time-points during treatment and showed a differential regulation of glycolysis (figure 18).

Name	48 hrs	3 wks
6-phosphofructo-2-kinase/fructose-2,6-biphosphatase 3	-6,5	-2,5
6-phosphofructo-2-kinase/fructose-2,6-biphosphatase	-2,6	+2,5
6-phosphofructo-2-kinase/fructose-2,6-biphosphatase 1	-2,8	n.c.
Hexokinase 3	-2,2	n.c.
Hexokinase 1	-1,6	+1,5
Hexose-6-phosphate dehydrogenase	-1,6	n.c.

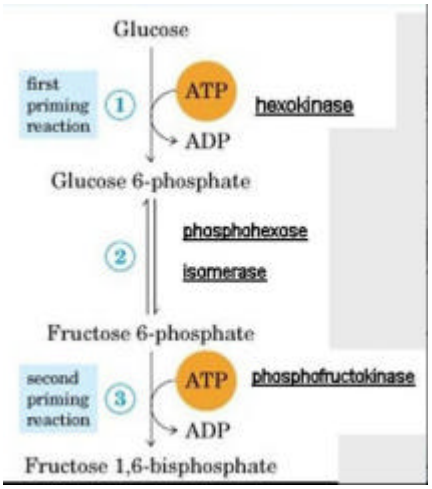

Figure 18: The table shows the gene expression of some enzymes important for the glycolysis. As can be seen, after 48hrs of tam-treatment all are down-regulated, while at 3 weeks everything returns to normal (n.c.=no change).

As can be seen in Figure 18, a strong down-regulation all three isoforms of phosphofructokinase occurred at 48hrs of treatment and was almost completely reversed after three weeks. Also an enzyme which is fundamental for the first priming reaction is down regulated at 48hrs as compared to three weeks of treatment. The determination of gene expression of enzymes important for oxidative metabolism did no such transient decrease (or increase for that matter).

3.1.7 Akt-induced hypertrophy is not accompanied by recruitment of new nuclei

Physiological muscle hypertrophy, e.g. during postnatal growth or following functional overload, induced by removal of synergistic muscles, is accompanied by proliferation of satellite cells, some of which subsequently fuse with associated fibers thus maintaining a normal nuclear domain size.

To assess the incorporation of new nuclei into tam-treated muscles, i.e. by activation of satellite cells, we injected mice for different time periods with Bromodeoxyuridine (BrdU), which is a synthetic thymidine analog that gets incorporated into a cell's DNA when the cell is dividing (during the S-phase of the cell cycle). One week after injecting 1mg of BrdU while activating Akt there was a clear increase in positive nuclei found in sections as compared to controls. To ascertain that these cells were actually incorporated into the fibers, sections were co-stained for laminin (figure 19a and b). This showed that only very rarely labeled nuclei were found inside the lamina.

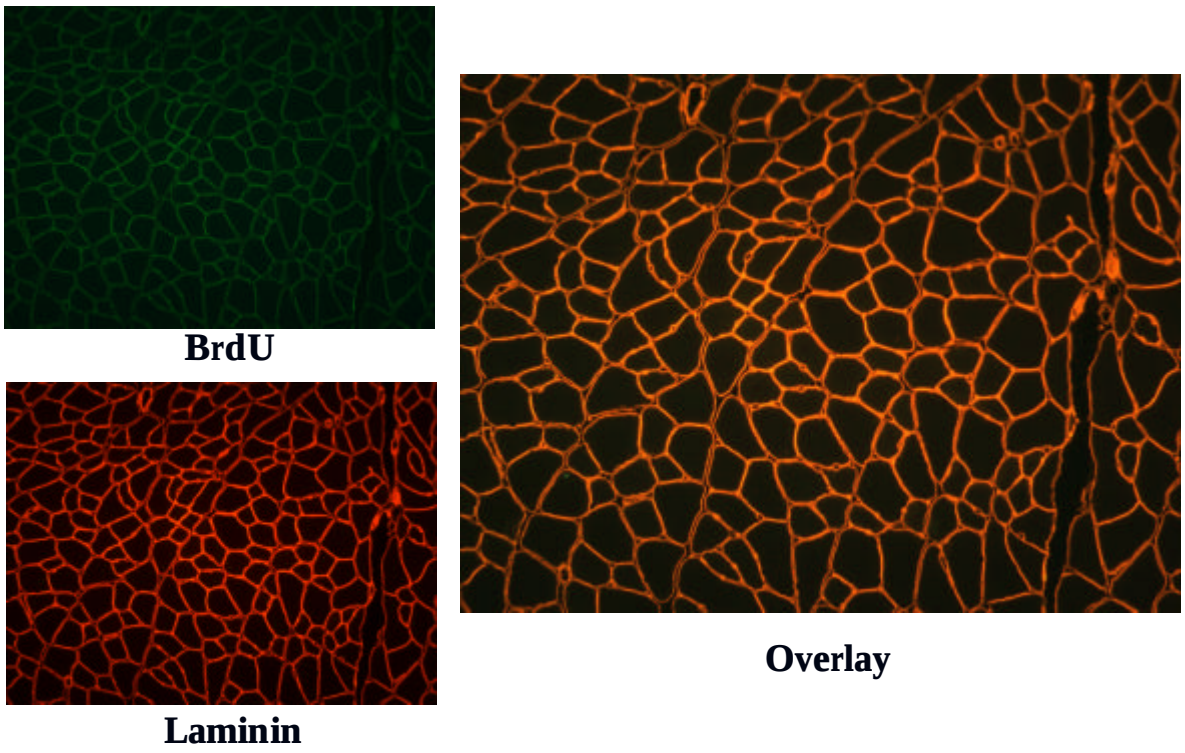

Figure 19a: No BrdU-positive nuclei are found in oil treated animals after one week of treatment. Animals were 3month-old females.

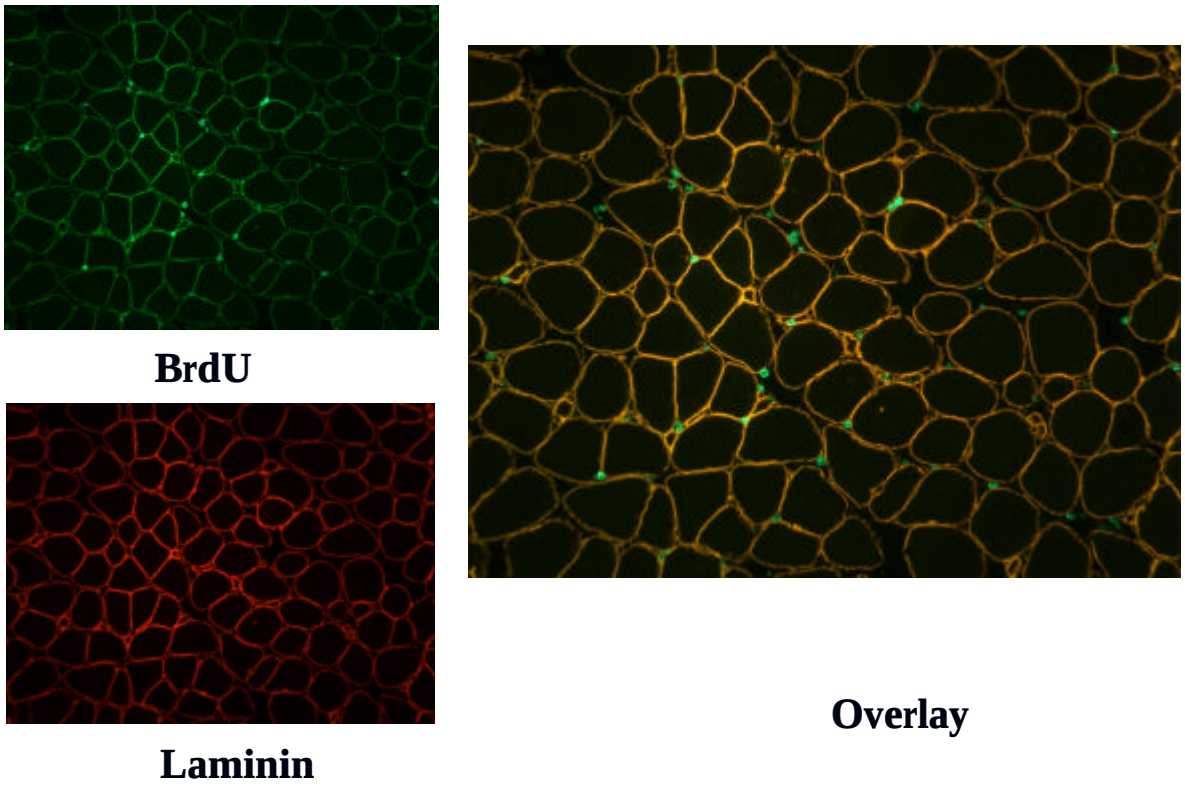

Figure 19b: One week treatment with tamoxifen every day leads to a strong cell proliferation, but positive nuclei were found only rarely inside the laminin staining.

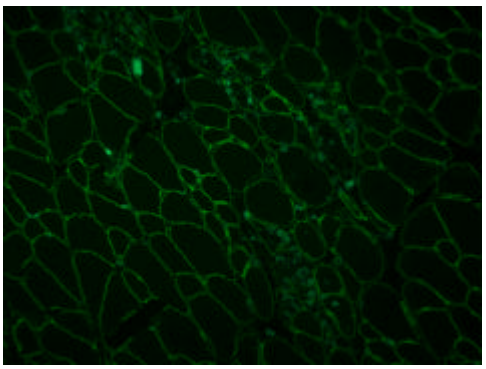

BrdU

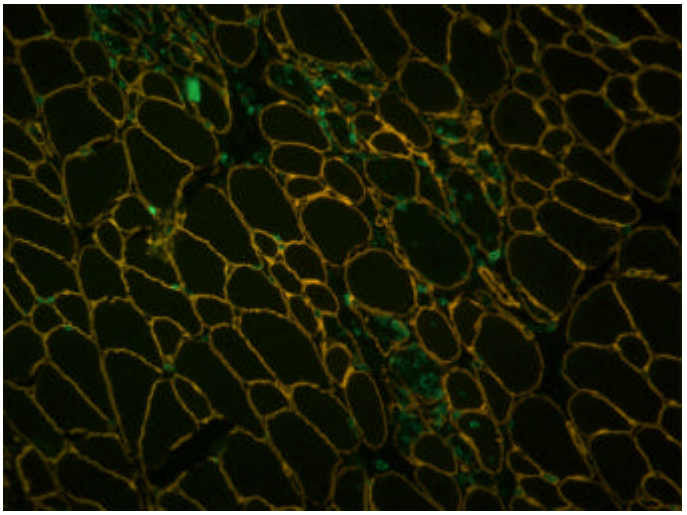

Overlay

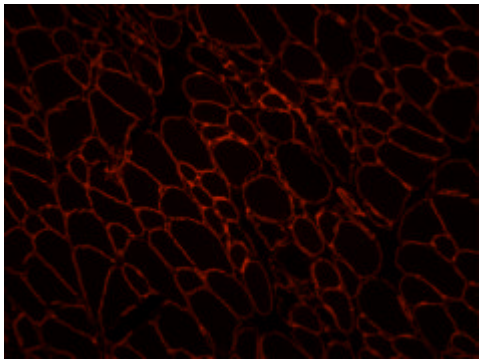

Laminin

Figure 19c: As a positive control for incorporation of BrdU-positive nuclei inside muscle fibers, we injected a 30 days old mdx for one week with BrdU every day. Even though the majority of positive nuclei are outside the fibers, there are several fibers with positive (central) nuclei.

In order to determine whether time was a key factor in this process we injected mice for three weeks with tamoxifen while simultaneously injecting them once a day with BrdU. The dose of BrdU in this protocol was reduced to avoid unwanted side-effects due to toxicity. As is shown in figure 20, some activated nuclei were found inside the fibers, but almost all remained outside of the lamina even after three weeks of treatment with tamoxifen, when from a metabolic point of view a steady state has been achieved. This gives strong indications that Akt does not induce strong proliferation and incorporation of new nuclei into already existing adult fibers.

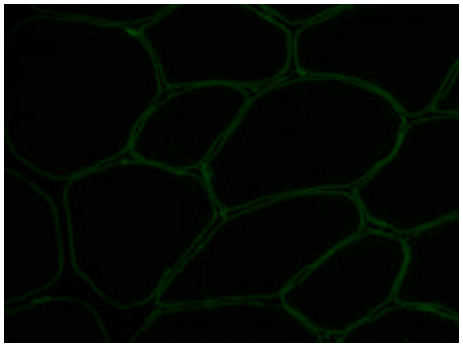

BrdU

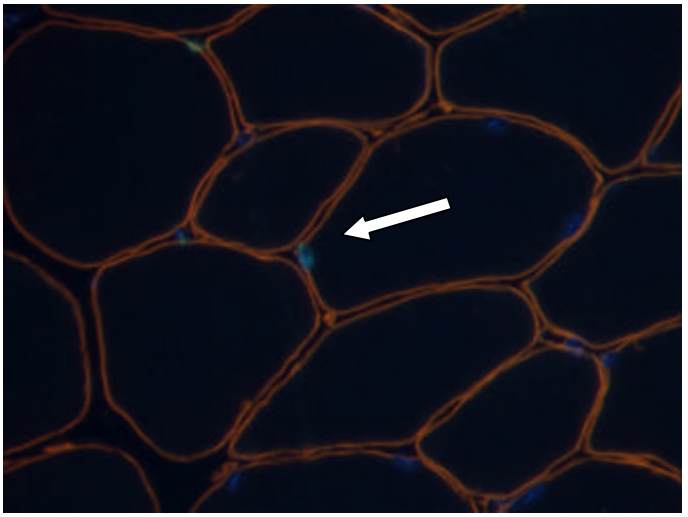

Overlay

Figure 20: After three weeks of injecting simultaneously tam and BrdU very rarely a positive nuclei was found inside the fibers. Almost all positive nuclei were found in the interstitial space.

Since incorporation of new nuclei during physiological growth could be a very rare event and therefore difficult to detect we decided to inject a 10 day old mouse for three weeks with BrdU. The incorporation of new nuclei after these three weeks, in which the developmental increase in muscle mass was similar to that observed in the Akt hypertrophic model, was clearly superior to that seen in the Akt hypertrophic model (figure 21).

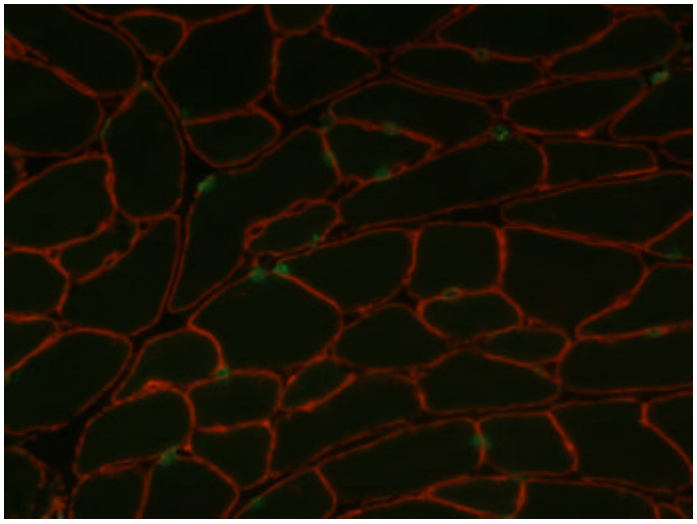

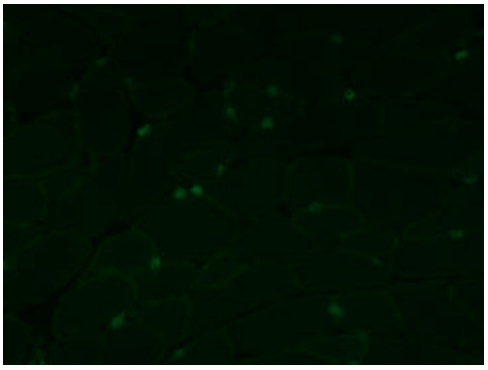

Figure 21: Incorporation of satellite cells during physiological growth is a regularly occurring effect.

3.1.8 Akt1 induces angiogenesis in vivo

The observation that hypertrophic muscles appeared more intensely red-colored led us to examine the amount of vascularization found in these muscles. Blood vessels can be distinguished in mature and immature groups, the former identified by smooth-muscle actin as a marker and the latter positively stained for CD105 or alkaline phosphatase. Staining for smooth muscle actin followed by a count of positive vessels showed a strong increase in mature vessels in hypertrophic animals (figure 22). The increase in number of mature vessels is about 60% compared to controls.

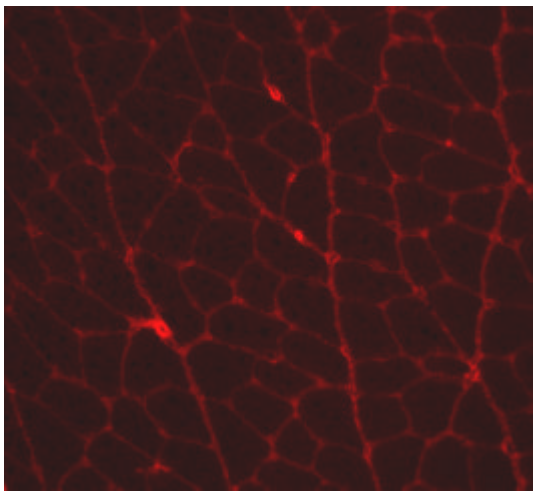

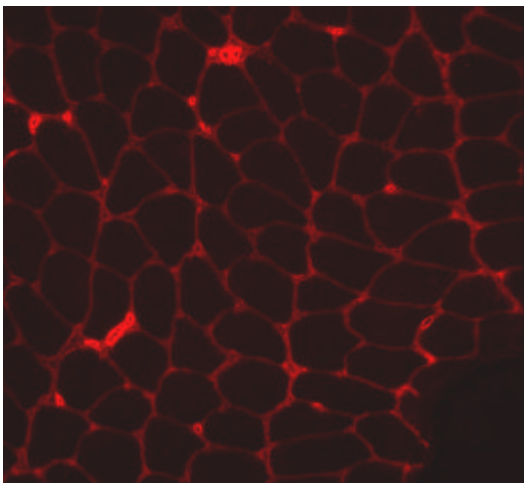

Oil **Tamoxifen**

Figure 22: Smooth-muscle actin staining shows the more mature blood vessels present in skeletal muscle. Quantification indicated that more vessels are present in tam-treated animals than in controls

Also multiple blots for myoglobin were performed, without consistently showing an increase in myoglobin content.

3.1.9 Effects of Akt-activation in spinalized and denervated muscle

To determine if Akt1, besides inducing hypertrophy, could also prevent atrophy and the corresponding force loss two models of atrophy were studied.
In the first model the spinal cord was transected around T8 leaving the animals paralyzed. After an initial flaccid phase spasms became more frequent. After three weeks of paralysis, while simultaneously injecting tamoxifen, a clear protection against the loss of muscle weight was seen (figure 23).

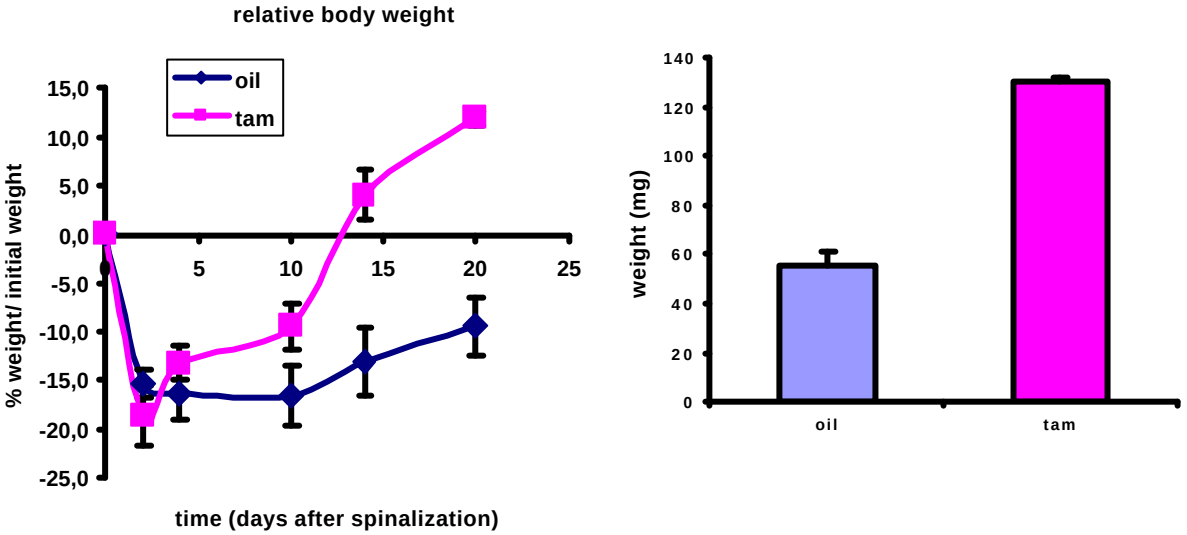

Figure 23: Body weight immediately after surgery decreased for both groups (left panel), but tam-treated animals recuperated the weight loss and showed no decrease in muscle weight. Muscle weight in tam-treated animals was markedly higher than in control animals (right panel).

In the second model mice were treated for one week with tamoxifen and oil, after which one of their legs was denervated. This operation is much less invasive for the animal, and therefore no great initial decreases in body weight were seen, even though a significant atrophy occurred in the gastrocnemius (figure 24).

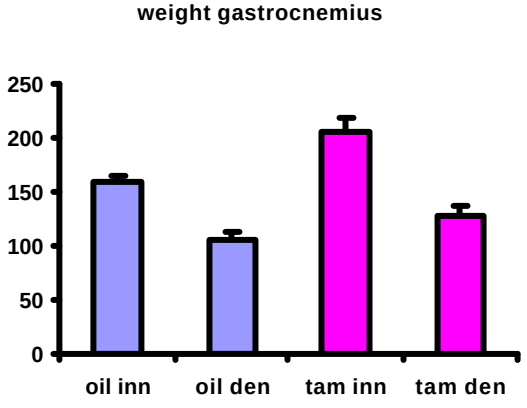

Figure 24: Muscle weights after one week of treatment followed by two weeks of denervation and treatment with tamoxifen.

Unexpectedly, the atrophy seen after two weeks of denervation was less pronounced than after three weeks of spinalization, and furthermore, akt1 activation was not able to completely protect the muscle against weight loss.
In order to evaluate if Akt cannot only avoid excessive loss of muscle weight in atrophic conditions, but is also able to rescue functionality of the muscles, in vivo force measurements were performed.
In the spinalization model the number of animals per group was four. Unfortunately two tam treated animals died in the latter stages of the treatment, and three oil and one tam-treated animal could not be stimulated through the sciatic nerve despite the presence of an esthetically healthy nerve. No force production could be measured in these mice, even when stimulating at highly elevated voltages.
The last of these mice (an oil-treated animal) which showed no response was stimulated with the electrodes placed directly on the gastrocnemius and showed force production values similar to those seen in the nerve-stimulated control animal.
The two animals that remained showed a clear functional protection of muscle function by Akt activation (figure 25). Despite a lack of numbers to back up this statement it can be seen as a clear proof of principle, akt1 can protect against force loss in a situation of spinalization atrophy.

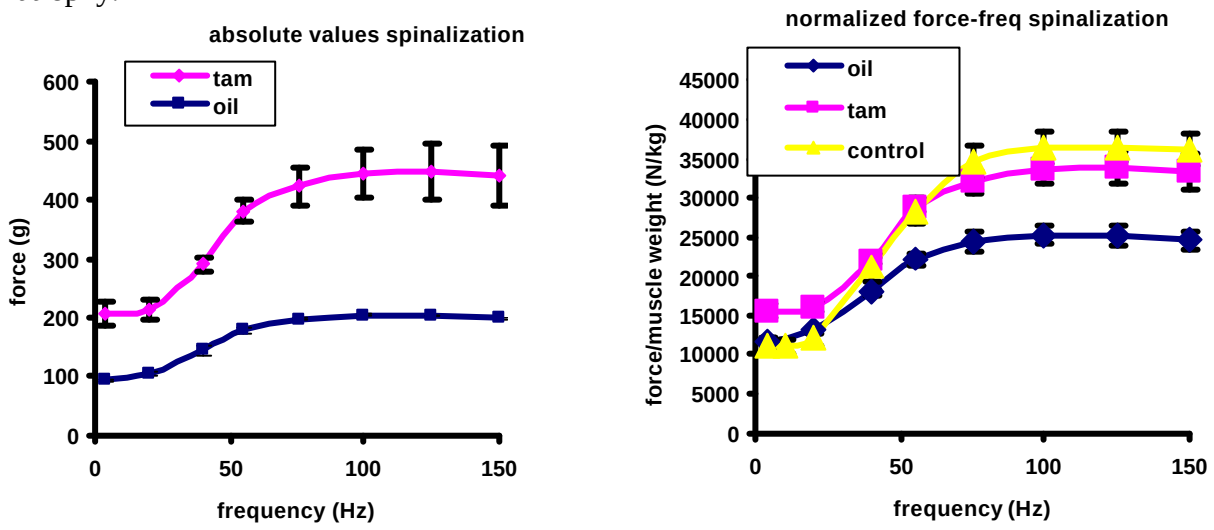

Figure 25: Tam-treated animals show a clear increase in absolute force compared to oil-treated animals. When normalizing for muscle weight tam-treatment keeps tension at control (wild type)-levels.

When looking at the denervation model, tam-treatment cannot rescue force production, since absolute force is even lower than in oil-treated animals (figure 26).

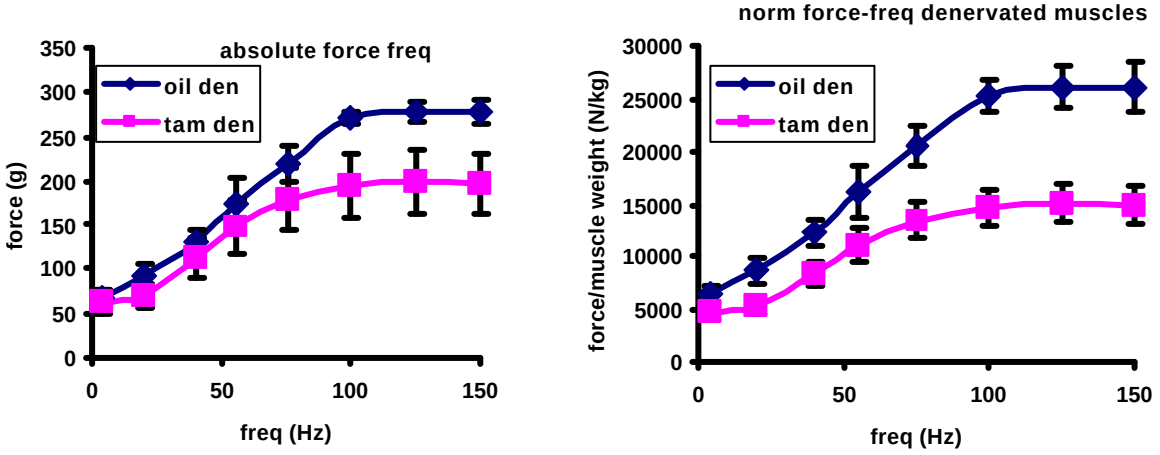

Figure 26: Both normalized as well as absolute force is lower in tam-treated denervated muscles than in controls.

Since it is known that in atrophic conditions there is a shift in optimal length, the force-length curve was determined (figure 27). From this graph it is very clear that optimum length in denervated muscles shows a leftward shift to higher muscle lengths, in both control as well as tam-treated animals.

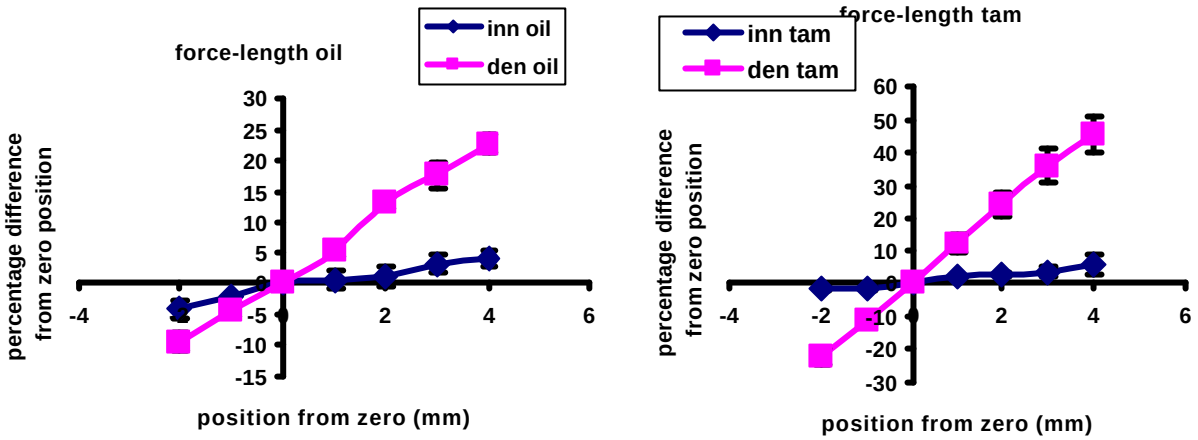

Figure 27: The force-length curves clearly show an increase in optimum muscle length after denervation, which in tam-treated animals is twice that seen in control animals.

All isometric force measurements from which the force-frequency curves are determined are performed at position zero. From figure it is clear that force measured at this position is giving values which are underestimating the maximal possible force production. The increase in absolute force production after increasing muscle length by 4mm is 23±1% in control animals, compared to 46±6% in tam-treated animals.

3.2 Effects of Akt-overexpression in dystrophic skeletal muscle (mdx)

3.2.1 Akt activation leads to skeletal muscle hypertrophy in mdx mice

Activation of Akt1 for three weeks leads to a significant muscle hypertrophy in dystrophic muscle (figure 1). However, the hypertrophic response seen in Akt-cre mdx mice was less pronounced than that seen in control transgenic akt-cre mice. Actually, hypertrophy in Akt-cre mice was about 50-60% after three weeks of treatment, while in Akt-cre mdx mice hypertrophy was never above 20%. Many qualitative features of the hypertrophic response were similar in mdx and normal mice as i) the hypertrophic growth was not dependent on fibre-type as both slow (soleus) as well as fast (tibialis anterior, EDL) muscle showed similar increases in muscle size, ii) the growth occurred mainly during the first week of treatment after which muscle weights tended to level off, iii) the hypertrophic effect was independent of sex as both males and females showed a similar muscle growth.

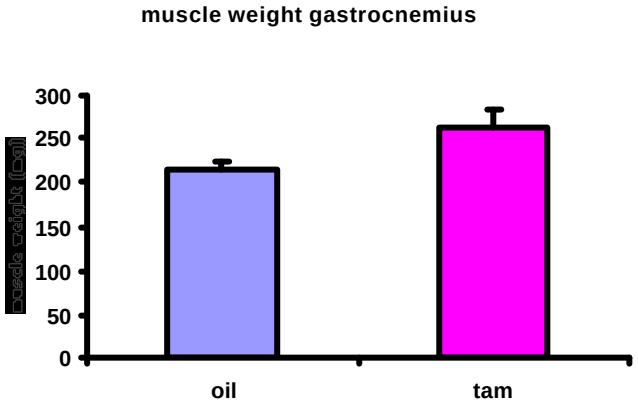

Figure 1: Three weeks of tamoxifen treatment leads to hypertrophy in all muscles examined. This graph depicts the weight increase in the gastrocnemius.

Dystrophic muscles, due to continuous regeneration, have a wide range of fibre diameters, ranging from very small, newly formed regenerated fibres, to very large hypertrophic fibres. Even though average fibre-size increased after akt-activation, this phenotype was not reversed (figure 2). Very small fibres remained present even after three weeks of Akt activation, indicating that degeneration-regeneration might be slowed, but surely not halted by Akt activation.

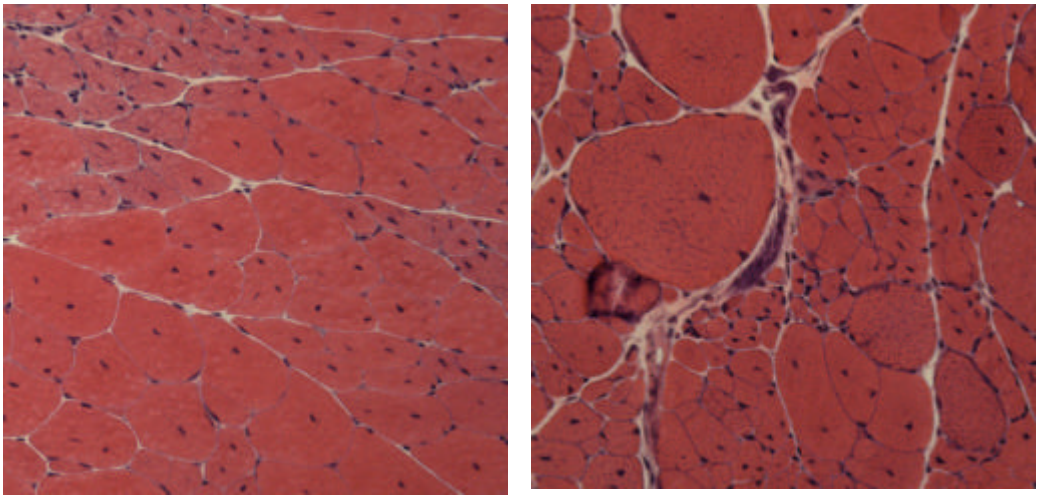

Figure 2: The pathological phenotype seen in dystrophic animals (central nuclei, infiltrations, variable fibre dimensions) is not reversed after three weeks of tam-treatment in Akt-cre mdx mice.

3.2.2 Muscle hypertrophy in Akt-cre mdx mice is not accompanied by an increased force production *in vivo*

In order to assess force production, hypertrophic muscles were stimulated through the nerve at different frequencies, ranging from a single twitch to a completely fused tetanus. The *in vivo* measurements of force development in the gastrocnemius showed no increase in absolute force. When the force was normalized for muscle mass, twitch tension was slightly, but significantly lower in hypertrophic animals. Due to a slight, but not significant increase in tetanic force in hypertrophic muscle, tetanic tension was not different between hypertrophic and control animals (figure 3).

It is important to underline that, despite repeated backcrosses (3rd generation), the background of the Akt-cre mdx mouse still contained a partial cd1 background, leading to higher normalized forces in the transgenic line than in normal mdx mice. Also body weights of the transgenic line were slightly higher than in normal mdx mice (data not shown).

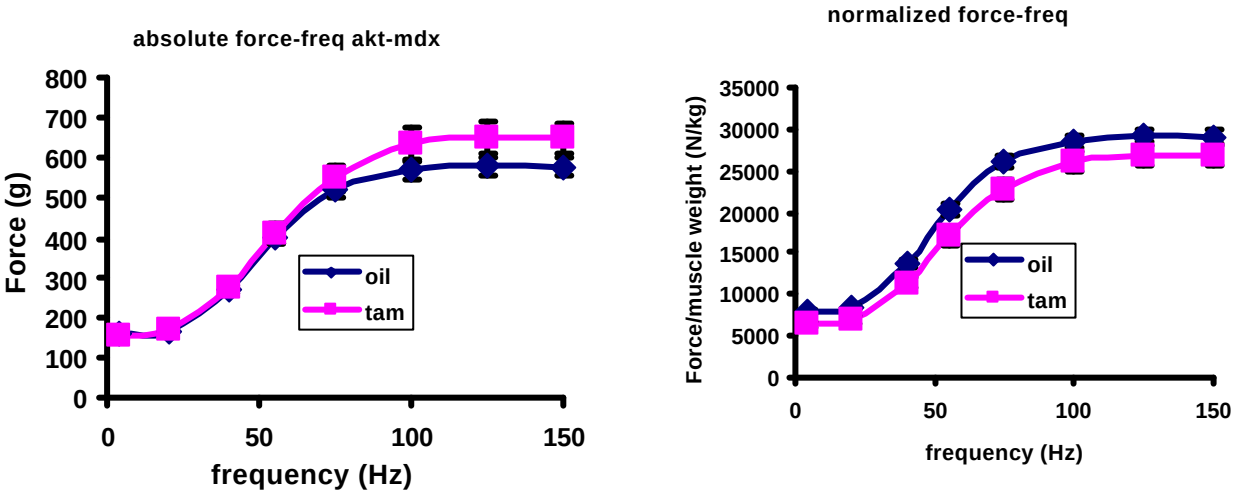

Figure 3: Akt activation does not induce any significant changes in force development, neither in absolute nor in normalized force in Akt-cre mdx mice.

3.2.3 Akt1 activation protects against lengthening contractions

It is well known that the decrease in force after a series of eccentric contraction is more pronounced in mdx than in normal muscles (Dellorusso et al., 2001; Petrof et al., 1993). In order to assess whether such increase sensitivity to muscle elongation was modified by Akt activation, series of eccentric contractions were performed on the gastrocnemius. The selected protocol based on 20 eccentric contractions caused in healthy c57bl6 mice a 14±1% decrease, which was significantly less than the 38±3% seen in the gastrocnemius muscles of mdx mice (figure 4). To ascertain that this decline was not due to metabolic fatigue, we repeated the same protocol of 20 stimulations without lengthening the muscle. This protocol did not lead to a decrease in isometric force (not more than 5%), neither in control nor dystrophic muscle.

When repeating these 20 lengthening contractions in the Akt1-cre mdx control group (mice receiving only the vehicle) we observed a decrease in isometric force, 34±4%, comparable to that seen in mdx mice. Interestingly, the phenomenon was not influenced by the higher isometric tension due to the mixed background.

Tamoxifen treatment for three weeks completely prevented the enhancement of the force drop induced by lengthening contractions typical of dystrophic muscle. After 20 eccentric contractions the force drop was 16±2%, essentially similar to values seen in normal muscle (not shown).

In order to assess whether this protective effect of Akt1 was related to the degree of muscle hypertrophy itself, we plotted the residual isometric force after 20 eccentric contractions

against a ratio which is indicative for the amount of muscle hypertrophy, namely gastrocnemius weight divided by body weight. Since Akt1 is exclusively activated in skeletal muscles, increased hypertrophy leads to an increase in this ratio as other organs remain unchanged in their size. In this plot (figure 5) no correlation is detectable between the hypertrophy and the protective effect of Akt1. Obviously, hypertrophic muscles tend to have a higher ratio, but it can clearly be seen that control animals with similar ratios show a clear force drop.

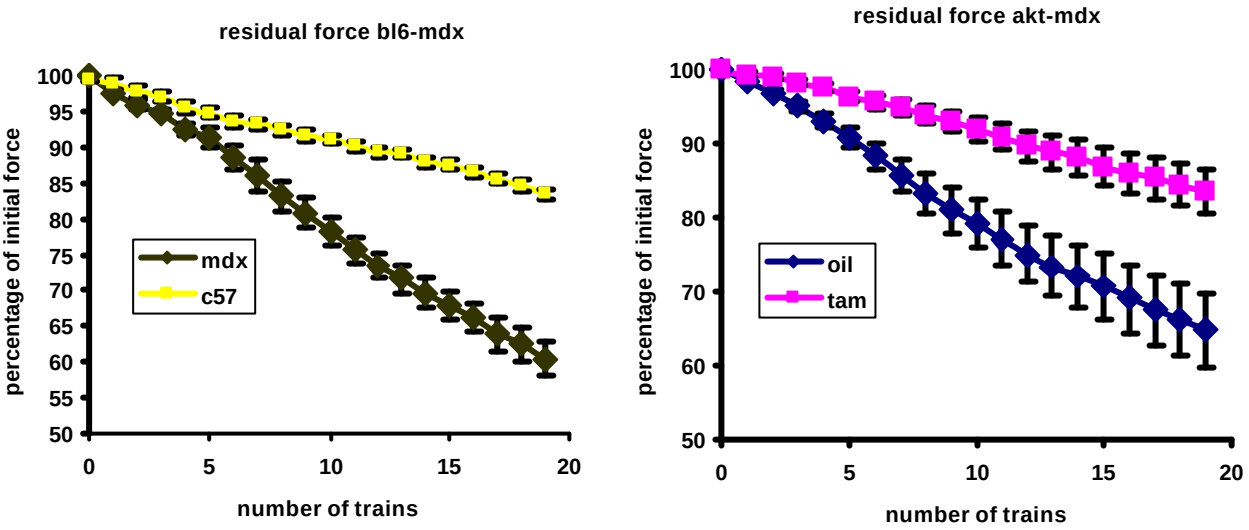

Figure 4: The decrease in force in mdx mice after eccentric contractions completely returns to control values after three weeks of treatment with tamoxifen.

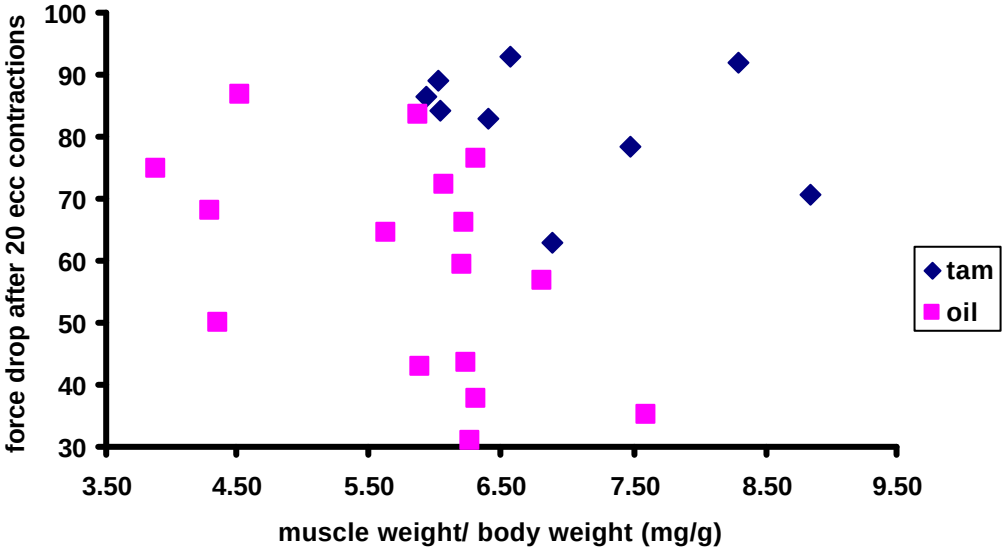

Figure 5: Muscle weight/body weight is an index for the amount of hypertrophy. As can be seen, no correlation is seen between the degree of hypertrophy and force drop induced by lengthening contractions.

3.2.4 Protective effect of Akt activation during lengthening contractions is independent of mTOR

To better understand the protective effect of Akt1 we examined if it was dependent on one of the main targets of Akt1 signalling, mTOR. Rapamycin is a drug which is highly specific in its inhibition of TOR-action. We therefore repeated experiments treating mice with either tamoxifen or oil, and during the last 8 days of treatment also administered rapamycin.

This experiment clearly showed that the protective effect is clearly independent of mTOR action during the last 8 days of treatment since force reduction after 20 eccentric contractions is 11±3% (figure 6).

As can be seen in the western blot performed on the gastrocnemius muscles from these mice, signalling downstream of mTOR is completely blocked as phosphorylation of S6, one of mTOR's main targets, is no longer detectable (figure 7). In order to exclude that this positive effect might be established by the two weeks of Akt1 activation preceding rapamycin treatment, we used a control in which we treated the mice for two weeks with tamoxifen followed by one week of oil treatment. In this case protection was indeed much less, the force decrease being 27±5%, slightly lower than in untreated mdx mice.

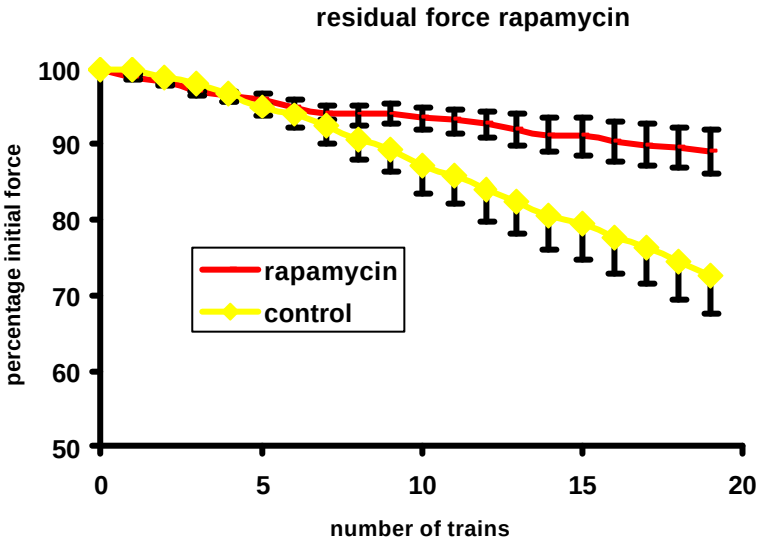

Figure 6: Rapamycin treatment does not block the protective effect of Akt-activation.

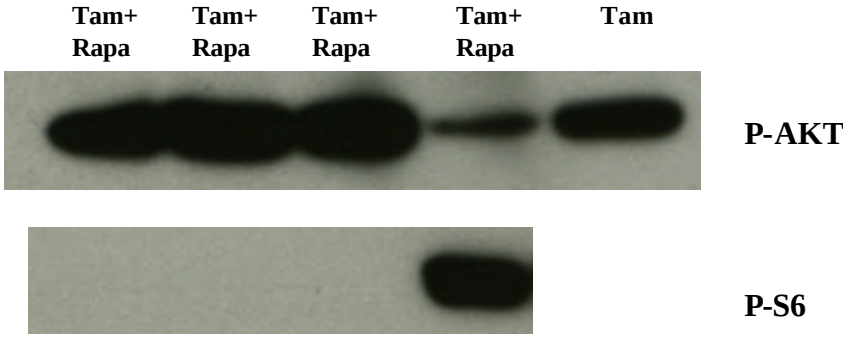

Figure 7: Rapamycin treatment completely blocks mTOR activation in tam-treated Akt-cre mdx mice, as shown by complete ihibition of phosphorylation of S6, detected by phospho S6-specific (p-S6) antibody.

3.2.5 Effects of Akt studied in skinned fibers

3.2.5.1 Akt protects against myofibrillar damage induced by lengthening contractions

To get a better understanding of the mechanism causing the force decrease induced by lengthening contractions in mdx mice, we examined the isometric force generated by single skinned fibres dissected from the gastrocnemius after performing eccentric contractions in vivo. We performed 20 eccentric contractions, using the same protocol as before, and immediately after placed the muscles is skinning solution. As a control we used fibres taken from the non stimulated controlateral leg. Measurements performed on these skinned fibers showed that the force developed by fibers taken from the eccentrically stimulated muscle (called 'damaged' from here on) was 34±12% lower compared to the force produced by fibers taken from the controlateral muscle (called 'control') (figure 8).

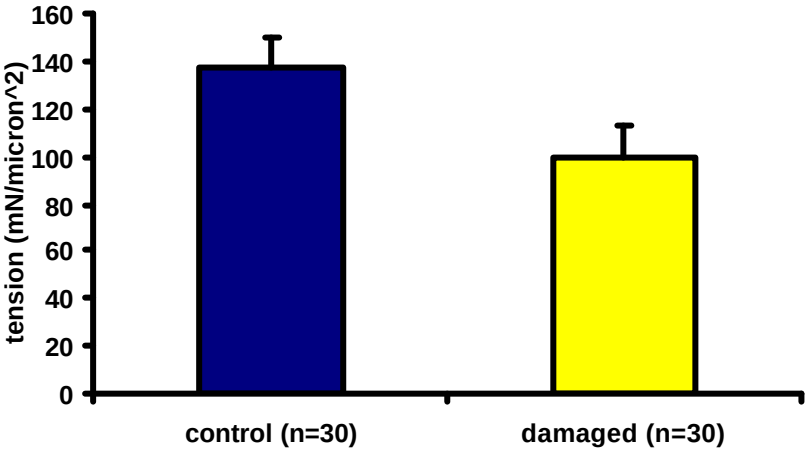

Figure 8: Eccentric contractions in vivo in mdx mice lead to a decreased force in skinned fibres, indicating myofibrillar damage

To examine if the protective effect of akt occurs on the myofibrillar level, we repeated the experiment using both oil and tamoxifen treated akt-mdx mice. Oil-treated animals showed the same difference between non stimulated and eccentrically stimulated leg as was seen in mdx mice (figure 9), whereas in akt-activated animals the force decrease was completely absent, indicating a protective effect of akt on the myofibrillar level.

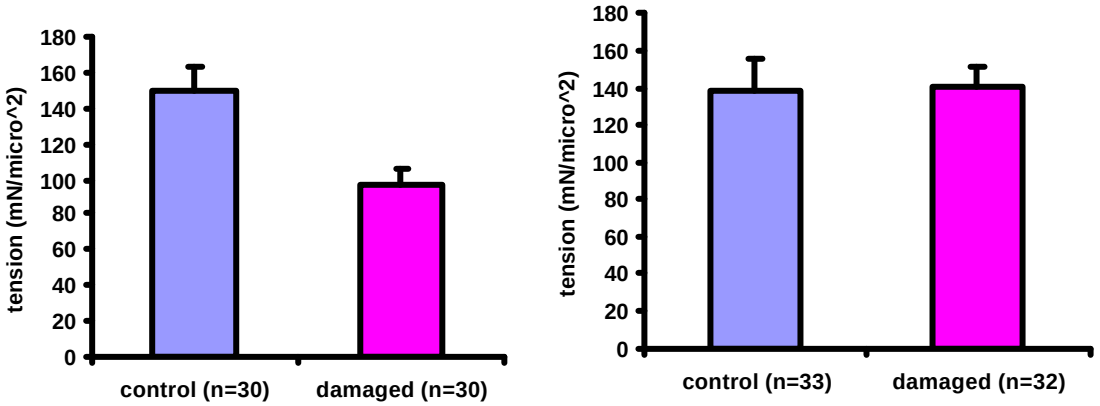

Figure 9: The force decrease in skinned fibres seen after eccentric contractions in vivo is completely avoided by three weeks of Akt-activation.

Interestingly, normalized force remained similar in oil-and tam-treated animals, despite a significant increase in fiber cross-sectional area in hypertrophic muscles (figure 10). This indicates that akt-activation lead to a hypertrophy which is completely functional when muscle fibres contract in vitro.

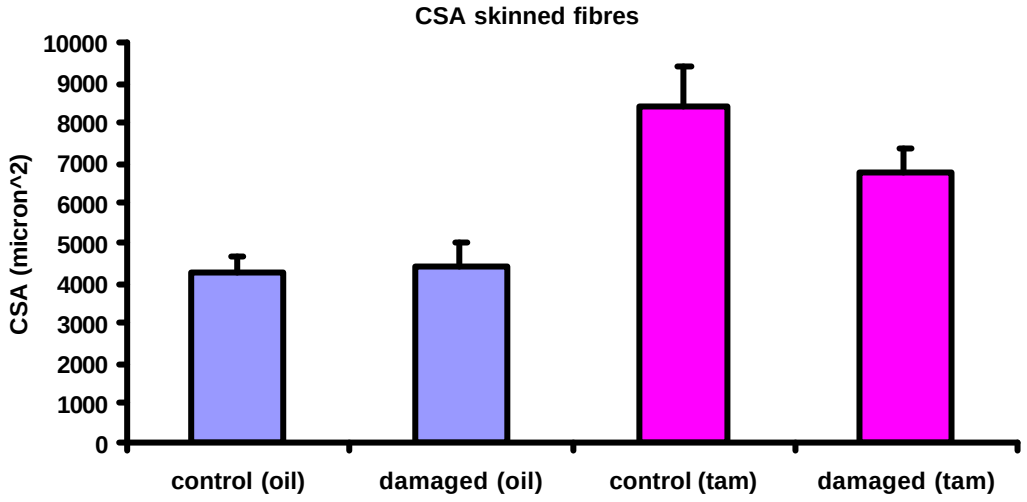

Figure 10: Skinned fibres taken from tam-treated animals showed a significant increase in cross-sectional area.

3.2.5.2 No difference in force deficits after eccentric contractions *in vitro*

To explore whether differences in isometric force deficits are due to stretching of the myofibrils per se, we repeated eccentric contractions in vitro and determined the force drop afterwards. After two eccentric contractions fibres from mdx mice showed a 21±6% decrease in isometric force (figure 11). This decrease was not significantly different from the 17±3% decrease seen in oil-treated akt-mdx mice.

Surprisingly, after three weeks of Akt-activation fibres showed a similar decrease, 16±2%, in isometric force. The lack of difference in the susceptibility to damage in skinned fibres indicates that myofibrillar damage is not due to a greater susceptibility of the myofibrils of dystrophic muscle, but to a change induced in vivo by eccentric contractions in the myofibrils.

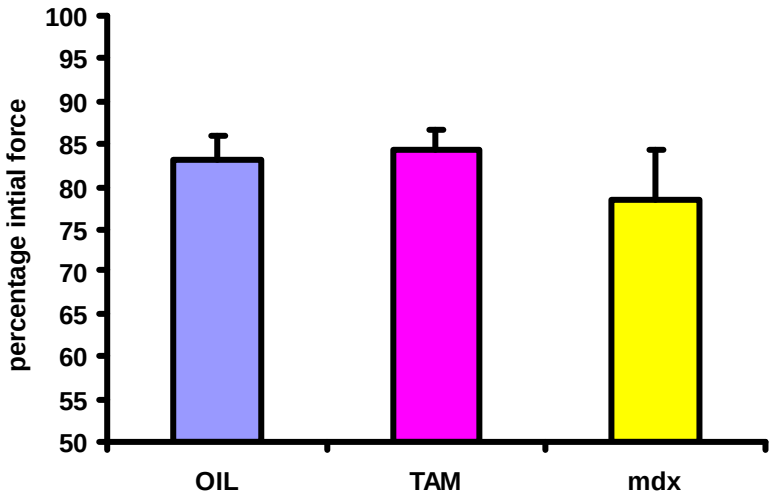

Figure 11: The force decline seen after two eccentric contractions in skinned fibres is similar in control and mdx fibres and is unchanged by Akt-activation.

3.2.6 Akt activation does not affect membrane permeability

We next examined the issue whether akt activation lead to a decrease diffusion of serum constituents inside muscle fibres. Due to sarcolemmal damage, a number of muscle fibres from mdx mice have elevated levels of albumin and IgG inside their muscle fibres. Blue Evans, by binding to albumin, is a commonly used marker to identify these fibres with a leaky membrane. When comparing dye uptake in untreated and tamoxifen-treated mdx mice we could clearly identify a different pattern of positive fibres. Whereas control mdx mice showed the typical distribution of groups of positive fibres, animals treated with tam showed mainly individual positive fibres (figure 12). However, no difference in the percentage of positive fibres between the two was seen.

Various groups have shown that the number of blue evans positive fibres increases after eccentric exercise. Muscles taken out immediately after eccentric exercise showed no change in the number of dye positive fibres, whether they were treated with tamoxifen or not (figure 13).

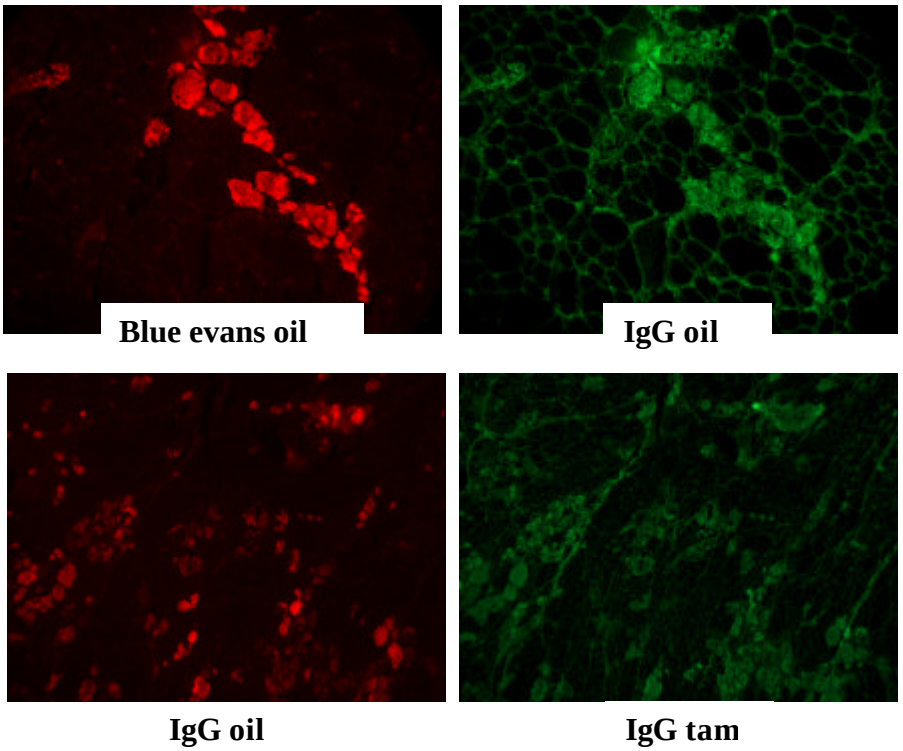

Figure 12: Evans Blue positive fibres (on the left) and fibre staining for IgG (on the right).

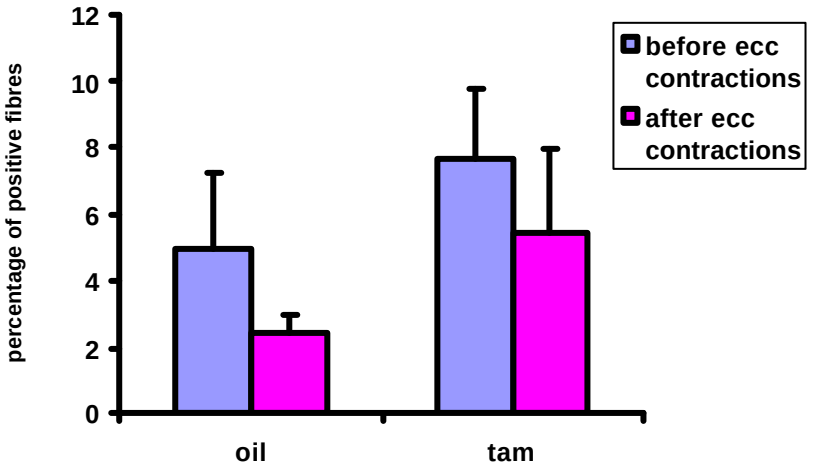

Figure 13: No significant changes in the number of Blue Evans positive fibres was seen, either before or after stimulation ù

A disadvantage of quantifying muscle damage by counting dye-positive fibres, is that only blue fibres which are present in the cryostat section are counted. An added problem is that this method gives an indication for one muscle at a time. To get a better evaluation of the overall increase in muscle membrane permeability, the amount of creatine kinase found in circulation is an eccelent method. In healthy mice the amount of circulating creatine kinase, a muscle specific intracellular protein, is below 500U/l. In mdx mice on the other hand, values are very variable and tend to be between 2000 and 10000 U/l.
To evaluate if Akt activation could reduce serum creatine kinase, we measured this parameter at various time-point, but found no significant difference between tam and oil-treated animals at any time (figure 14).

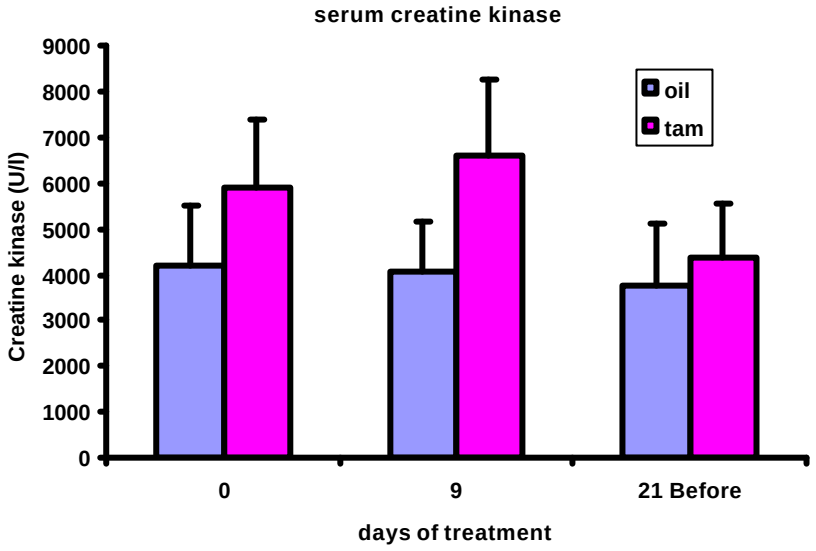

Figure 14: Creatine kinase content in the serum is unchanged during oil and tam treatment.

3.2.10 Calcium homeostasis is unchanged by Akt activation in mdx mice

In order to clarify if the force drop induced by eccentric contractions could be due to a defective excitation-contraction coupling, we measured the calcium transient in single fibers taken from the flexor digitorum brevis. To elicit a twitch the fibers were electrically stimulated at low frequencies (below 5 Hz). Calcium transients were determined using a fura-2 dye, which emits light at two different wavelengths, depending on whether its bound to calcium or not. The results clearly show no difference between oil and tam-treated animals, showing a functional excitation-contraction coupling in hypertrophic fibres (figure 15). We also determined the baseline signal for the fura-2 and the time parameter of the transient, but we could not detect any differences there either.

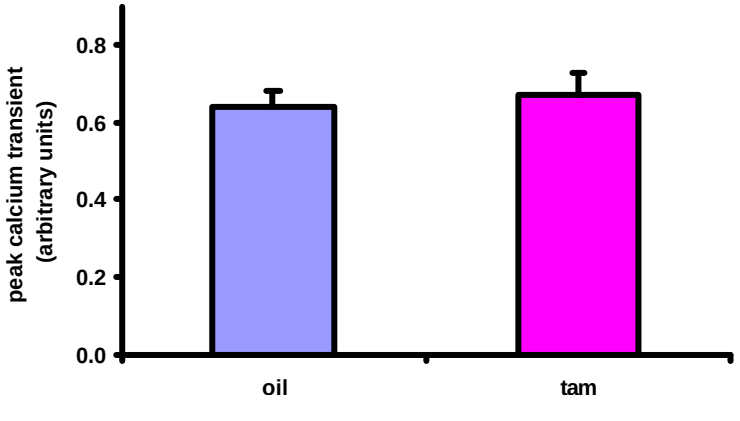

Figure 15: No difference in peak calcium transient between tam-treated and control animals.

3.2.8 Akt activation does not restore dystrophin expression

It has been suggested that blocking of the proteasome could lead to the expression of a truncated form of dystrophin in mdx mice (Bonuccelli et al., 2007). This truncated protein contains the N-terminal domain of the dystrophin protein and is transcribed up to the premature stopcodon, which is responsible for the absence of dystrophin protein in mdx mice. To verify if this truncated form of dystrophin is expressed in treated mice we stained cross-sections of the gastrocnemius muscle with an antibody specific for the N-terminal domain of dystrophin. As can be seen in figure 16, no difference could be detected between the two groups. Apart from the occasional revertant fibres, which were present in both groups, there was no positive staining of the membrane in most fibres.

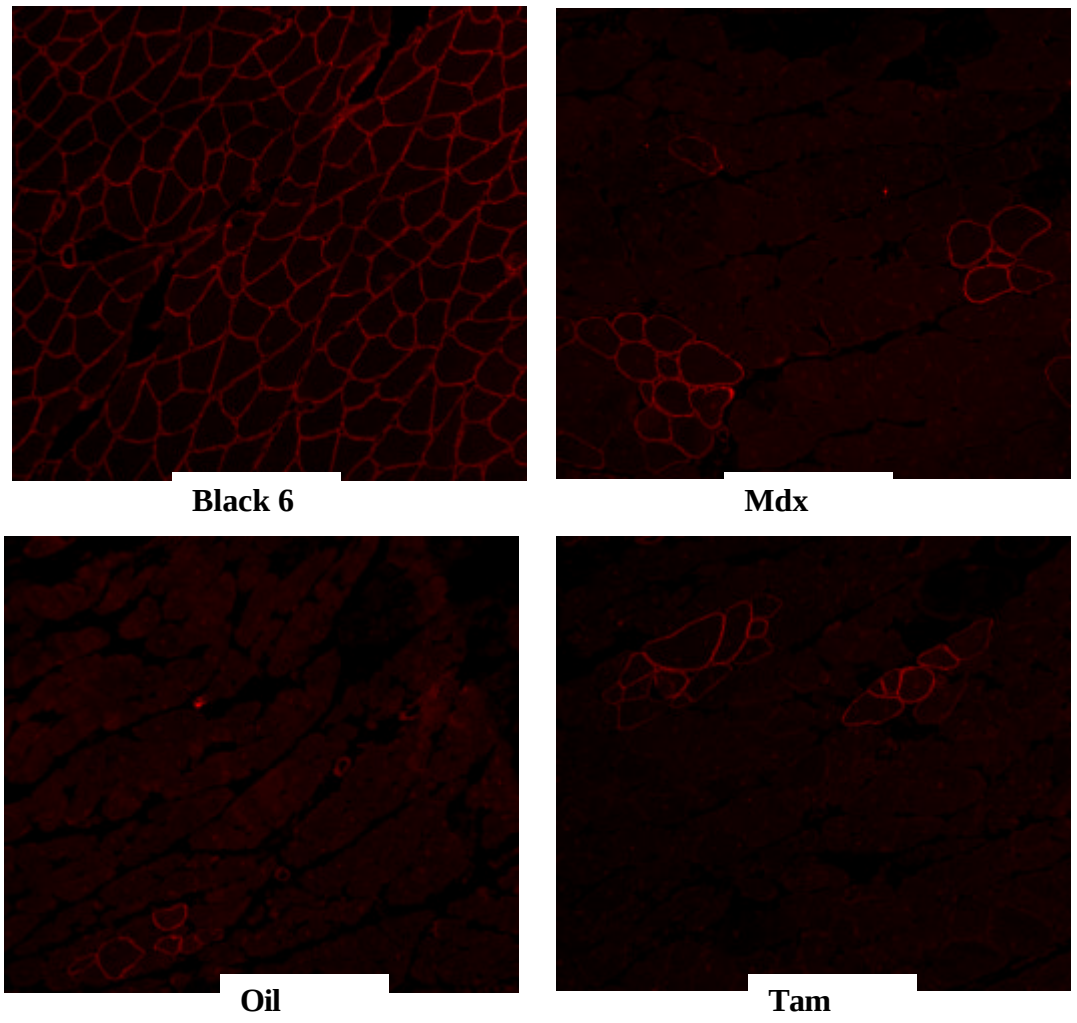

Figure 15: Staining for N-terminal domain of dystrophin showed no increased dystrophin content after Akt-activation. Only some revertent fibres could be detected.

3.2.11 Increased utrophin and desmin content after Akt-activation

To determine if the protective effect during eccentric contractions could be due to a reinforced cytoskeleton, we performed western blots to determine the desmin content. Desmin is a well known protein specific for intermediate filament, which is thought to play an important role in

preserving the structural integrity of the fibre As shown in figure 16, Akt-activation leads to a two-fold increase in desmin content in tam-treated animals, as assessed in Western blots.

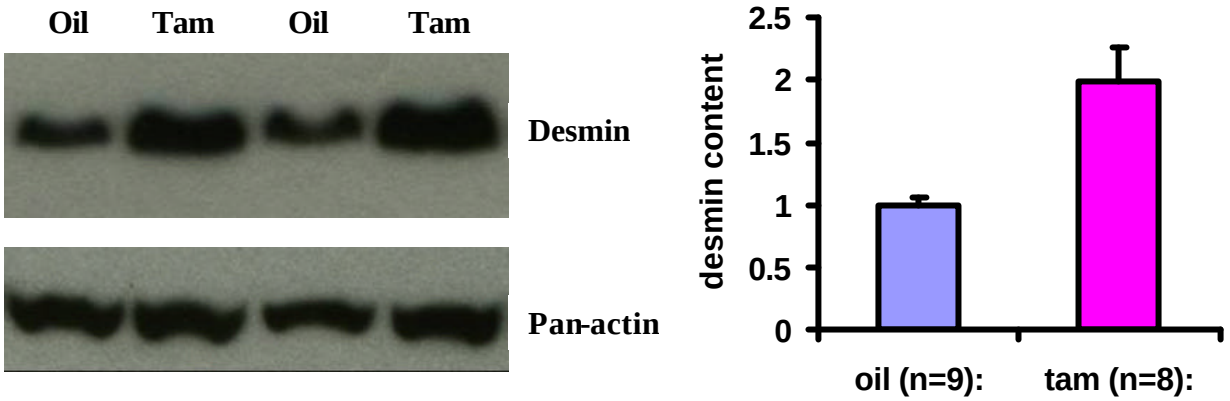

Figure 16: Desmin content doubles after three weeks of Akt-activation

Utrophin is the autosomal homologue of dystrophin, and like dystrophin interacts with the cytoplasmic domain of β-dystroglycan. Mdx mice are known to have an increased amount of utrophin at the fibre membrane, as opposed to healthy mice where utrophin is only localized in the neuromuscular junctions. When transgenic mice over expressing utrophin are crossed with mdx mice a complete recovery from all pathological signs was observed. In order to determine if the protective effect during eccentric contractions could be due to an increased amount of utrophin we performed a real-time PCR to determine the mRNA-levels of utrophin (figure 17).

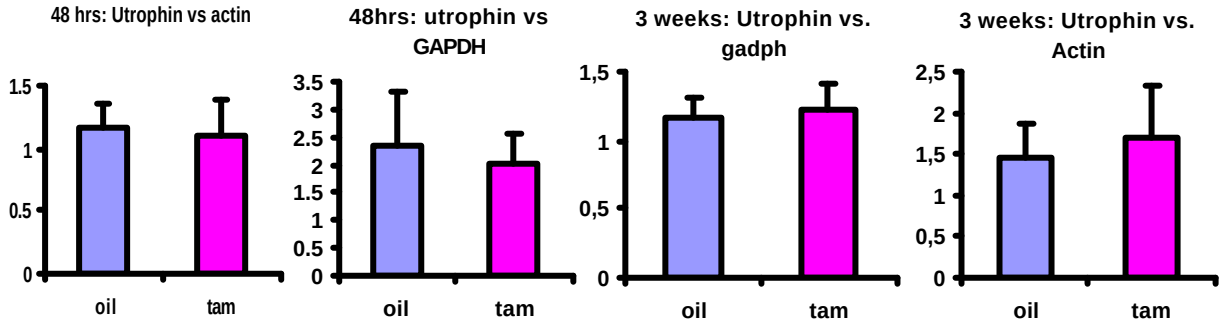

Figure 17: mRNA-levels of Utrophin, as determined by real-time PCR using two different house-keeping genes, do not change during the course of the treatment.

Utrophin was not transcriptionally up regulated in tam treated mice, therefore we checked if the amount of the protein was increased through post-translational modifications. By using a monoclonal antibody we performed an immunohistochemistry which seemed to indicate an increased expression (figure 18). However, the amount of background made difficult to interpret the images.

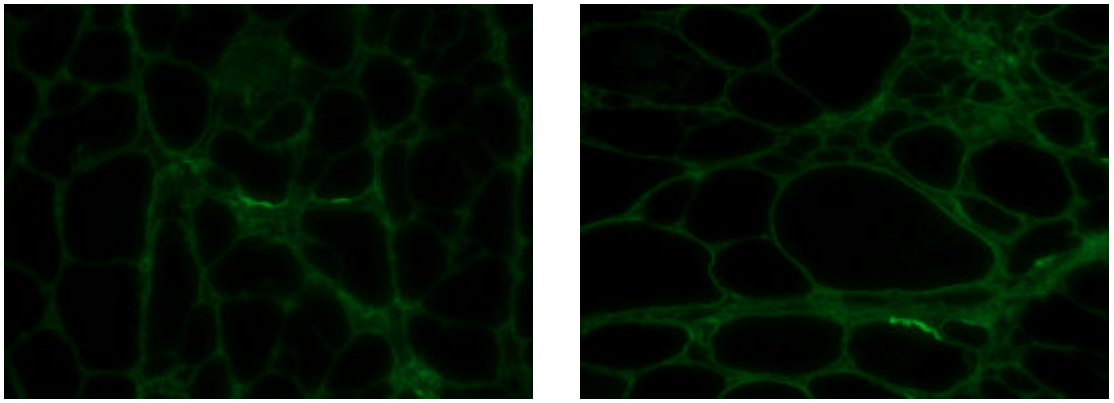

Figure 18: Immunohistochemistry for utrophin showed a sharper delineation in tam-treated fibres, suggesting increased utrophin content. Note the strong staining in the neuromuscular junction.

By western blotting, we found a clear increase in utrophin content after three weeks of akt-activation (figure 19). Quantification of these blots suggested that the increase was between two-to threefold of the level seen in control animals.

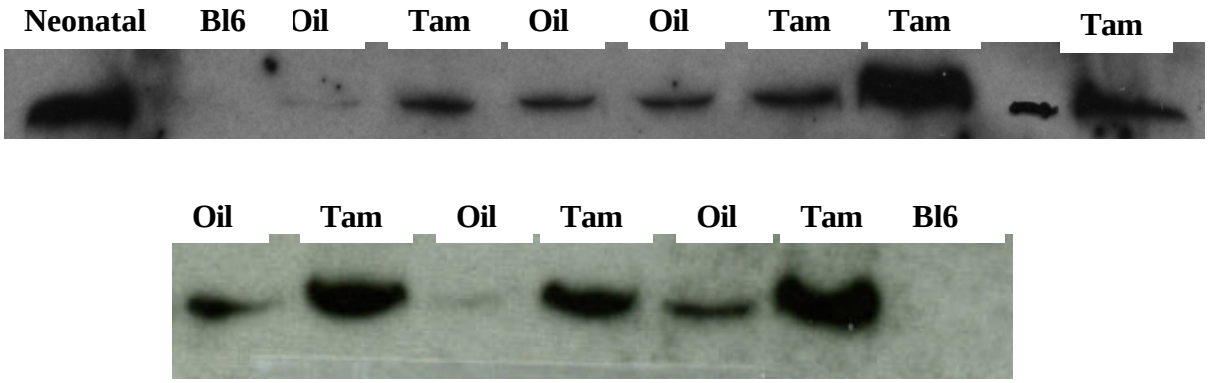

Figure 19: Two western blots showing a clear increase in utrophin content after three weeks of tam-treatment.

4. Discussion

4.1 Effect of Akt activation in normal muscle

4.1.1 Skeletal muscle hypertrophy induced by Akt

In the present study we show that activation of Akt is sufficient to induce skeletal muscle hypertrophy, as in agreement with previous studies (Lai et al., 2004; Pallafacchina et al., 2002). The increase in fibre-size is likely due to activation of mTOR, that leads to an increased protein synthesis, and by inhibition of FoxO transcription factors reducing protein breakdown via the ubiquitin-proteasome (Sandri et al., 2004) and autophagy-lysosome pathway (Mammucari et al., 2007). Akt activation only leads to an increased muscle mass, without changes in fibre type.

Our studies show that muscle hypertrophy induced by Akt is a functional hypertrophy as shown by an increase of muscle strength *in-vivo*, improved actin-myosin interaction, and an increased calcium release.

4.1.2 Functional properties of hypertrophic muscles

These results can be compared with two other models skeletal muscle hypertrophy, that induced by the loss of myostatin and that induced by insulin like growth factor 1 (IGF-1).

Mice over-expressing a local form of insulin-like growth factor 1 (mIGF1) showed an increase in absolute force which was in proportion to the increase in muscle mass (Musaro et al., 2001). Transgenic mice which completely lack myostatin, on the other hand, show a strong hypertrophy, but no increase in absolute force and a strong decrease in normalized tension (Amthor et al., 2007).

In the present study we clearly show that activation of Akt1 is sufficient to induce a functional skeletal muscle hypertrophy. However, an increase in muscle force *in-vivo* is not proportional to the increase in muscle mass. This discrepancy with the IGF-1 transgenic model can be explained by the change in pennation angle as the muscle growth is much more rapid than the growth of the tibia (no length changes observed) and therefore implies a radial expansion of the muscle. Indeed, when examining strips of the diaphragm, which has almost no pennation angle, the increase in muscle force is in proportion to the increase in muscle mass. The functional difference between the hypertrophy induced by IGF-1 and Akt could be explained by the fact that the measurements on the IGF-1 model were performed ex-vivo on the EDL, and the muscles used for physiological evaluation showed a very mild hypertrophy (only ±20%). In our model physiological assays were performed on different muscles which had undergone a much greater hypertrophy (±50%). In a moderate hypertrophy as that used for force measurements in the IGF1-study, changes in pennation angle are likely to be have been of less importance

4.1.3 Functional studies on skinned fibres

Evidence for increased force generation by hypertrophic muscles was also obtained by studies on skinned fibers. In these skinned fibers even the normalized force was significantly increased in hypertrophic compared to control animals. As is well known, fibres swell when placed in skinning solution. When comparing the fibre diameter in freshly cut sections to the diameter found in skinned fibres we clearly see a reduced swelling in tamoxifen treated fibres compared to control fibres. Such reduced swelling can partly explain the greater tension seen, since cross-sectional area increases less in hypertrophic fibres than in control fibres upon permeabilization with skinning solution. Indeed, hypertrophic skinned fibers taken from human body builders show an increase in tension (D'Antona et al., 2006), which can be explained by an increased rigidity of the cytoskeleton that opposes the swelling. The authors

find a significantly smaller increase in average fibre diameter than would be necessary to explain the whole muscle hypertrophy, +14% versus +54%. Also noteworthy is that this discrepancy is no longer present when a muscle biopsy is immediately frozen and fibre diameter is determined on cryostat sections (Esmarck et al., 2001). It is tempting to speculate that these muscles, which regularly are subjected to great stresses, undergo remodelling of the cytoskeleton in order to withstand the great loads placed upon them. Akt1 could be a candidate in stimulating this reinforcement of the cytoskeleton as Akt is known to be stimulated by muscle contraction (Sakamoto et al., 2002) and cytoskeletal organisation is dependent on remodelling of cytoskeletal proteins (Bezakova and Lomo, 2001).

4.1.4 Calcium transients in hypertrophic fibres

In order to determine whether skeletal muscle fibres also show an increased calcium release after activation of Akt1 we looked at the transients of isolated muscle fibers after 3 weeks of Akt1 activation. Hypertrophic muscles indeed showed increased peak calcium transient after electrical stimulation, which was in proportion to the increase seen in fiber-volume after isolation from the flexor digitorum brevis muscle. Transient times were unchanged, indicating an increase in number of calcium channels as well as pumps, as has been reported in mice over-expressing a constitutively active Akt1 in the heart (Kim et al., 2003), (Rota et al., 2005). This increase in peak transient elicited by a single twitch is confirmed by the increase in twitch force. Twitch forces though showed an increase in twitch times which cannot be related to changes in calcium kinetics.

4.1.5 Cell proliferation in hypertrophic muscles

In other models of muscle hypertrophy, including potsnatal muscle growth, the increase in size of muscle fibres is accompanied by proliferation of satellite cells and their incorporation into the neighbouring fibres. In this way the nuclear domain within the fibres, i.e. the cytoplasm to nucleus ratio, remains constant. However, our BrdU incorporation studies show that in hypertrophic muscles most labeled cells were found in the interstitium, while very few were incorporated into mature fibers after 3 weeks of Akt activation. Thus, it seems that Akt is mainly involved in the growth of muscle fibres without affecting proliferation and incorporation of satellite cells. It does therefore lead to an increased nucleus-to-cytoplasm ratio, at variance with models in which specific force is maintained, like functional overload and testosterone treatment (Roy et al., 1999). The decrease in normalized force seen *in vivo* could therefore in theory be due to this increased nuclear domain. It is thought that transport distances and the capacity to synthesize proteins could suffer from a decrease in nucleus-to-cytoplasm ratio (Bruusgaard et al., 2005). The ski-induced hypertrophy shows increases in the nuclear domain together with a reduction in contractile material and misalignment of Z-lines. Since the 30% decline in specific force seen in these animals can almost completely be explained by this reduction in contractile material, it is unlikely that the decrease in normalized force seen in Akt-induced hypertrophy is due to an increased nuclear domain. To examine if the lack of incorporation of new nuclei is due to the model studied, i.e. mature muscle fibres, we have decided to treat young akt-cre mice (15 day old) for three weeks with tamoxifen, and in the last week of treatment also with BrdU. This showed (results not shown) no difference in BrdU-incorporation between treated and control animals, despite a clear hypertrophy, also in these already growing muscles. This confirms that our model of activation of myr-Akt is not accompanied by activation of satellite cells, even in young mice.

4.1.6 Effect of Akt activation during atrophy

In order to evaluate the effect of Akt in conditions of atrophy a model of spinal transection and a model of denervation have been used. Both of these models mimic conditions of atrophy due to muscle disuse, even though the former is a good model of inactivity, while the latter leads to degeneration of the nerve, depriving the muscle of potential trophic factors and inducing changes in muscle membrane properties (Midrio, 2006).

Surprisingly, the atrophy seen in the spinalization model is more pronounced than in the denervation model (Leblond et al., 2003; Sacheck et al., 2007). This is unexpected since spinalization leads to a spastic paralysis after an initial flaccid phase, as compared to a flaccid paralysis in denervation (with some early fibrillations).

Akt1 leads to a complete rescue of muscle mass in the more severe spinalization atrophy, while the rescue is more modest in the denervation model. These differences might be due to subtle differences in expression profiles found in different atrophies (Sacheck et al., 2007). Actually, the functional protection in the spinalization model is detectable only in those muscles that can respond to electrical stimulation, as many didn't respond, despite any visible nerve defects. Both absolute as well as normalized force is higher in treated as compared to control animals showing the capacity of Akt1 in avoiding the loss of muscle function in spinalization atrophy.

In the case of denervation atrophy, Akt1 seems to be unable to completely protect against the loss of muscle weight and showed reductions in both absolute as well as normalized force. A partial explanation for this force reduction is that measurements were performed at non-optimal muscle lengths.

Interestingly, atrophic muscles show a big shift in optimal length, i.e. the length at which force production is maximal, towards a bigger optimum length. This means that force measurements are not performed at the best position and therefore maximal force production can be greatly underestimated (at least 30%). The shift towards a greater optimum lengths is twice as big in tam-treated muscles increasing the underestimation in this case even more. It is known that very pennate muscles add sarcomeres in series when they go into atrophy, yet this doesn't explain why optimum length should increase and neither why this increase does not occur in the spinalized model.

4.1.7 Conclusions

In summary, this study clearly demonstrates that Akt1 activation in mature skeletal muscle is sufficient to induce increases in muscle size and strength, calcium release, blood vessel formation, actin-myosin interaction, all while retaining a normal ultra structural organization. All evidence points to Akt1 as being a key protein in inducing not only hypertrophy, but also leading to improved muscle function. This study shows the great therapeutic potential of the Akt1-pathway in inducing bigger and stronger muscles.

4.2 Effects of Akt activation in dystrophic skeletal muscle

We found that Akt-over expression leads to a rapid hypertrophy in mdx mice. Importantly, three weeks of Akt activation lead to a complete protection against force loss due to lengthening contractions in dystrophic skeletal muscle, and this effect is independent of hypertrophy per se. The force loss following lengthening contractions, to which dystrophic skeletal muscle is particularly susceptible, is due to changes of myofibrillar components and activation of Akt is sufficient to prevent these changes. It is possible that the protective effect of Akt is mediated by upregulation of utrophin, the homologue of dystrophin, and of another cytoskeletal protein, desmin.

The concept of battling the muscle wasting and muscle weakness seen in muscular dystrophy by increasing muscle mass has been suggested previously (Barton et al., 2002; Bogdanovich et al., 2002). Blocking of myostatin leads to an increased muscle mass, body weight, and absolute muscle force (Bogdanovich et al., 2002; Bogdanovich et al., 2005). However, myostatin blockade did not protect against damage from lengthening contractions. In studies on transgenic mice over-expressing IGF-1 in skeletal muscle an increase in muscle strength, regenerative capacity and a decrease in muscle necrosis is found (Barton et al., 2002; Musaro et al., 2001). Also an improved excitation-contraction coupling (Schertzer et al., 2007) and a partial protection against lengthening contractions can be achieved (Barton et al., 2002; Schertzer et al., 2006).

4.2.1 Akt activation leads to skeletal muscle hypertrophy, but is not accompanied by an increase in force

The activation of Akt leads to a rapid hypertrophy in mdx, albeit less pronounced than that seen in normal mice. The lower degree of Akt-induced hypertrophy in Akt mice may be due to the fact that dystrophic muscle is already hypertrophic per se before treatment. Such hypertrophic response present in mdx mice is considered to be due to an activation of the Akt-pathway (Peter and Crosbie, 2006). In contrast with the other models discussed above, the hypertrophy induced by Akt-activation in mdx mice is not accompanied by an increase in absolute force. This difference with the two other models can be explained by the difference in the age of the animals when hypertrophy was induced treatment time and duration of treatment, or the different signalling pathways activated in the various models. In our model, two-to three month old mice, which already present all the pathological signs of dystrophy, are treated for three weeks before physiological evaluation. Indeed, IGF-1 over-expression in 9-month old mdx mice does not produce any increase in muscle force (Abmayr et al., 2005) and this is at variance of the transgenic model over-expressing Igf-1 from birth (Barton et al., 2002). In the myostatin model mice are treated for three months, starting at 4 weeks of age (Bogdanovich et al., 2002; Bogdanovich et al., 2005). In addition, in the myostatin model other signalling pathways are activated.

4.2.2 Akt activation protects mdx mice from the force drop following lengthening contractions

The most important finding in the study of Akt activation in mdx mice is that dystrophic muscle are protected against the force drop following lengthening contractions. The reason for the increased susceptibility of dystrophin deficient muscle to lengthening contractions is still a debated issue. A problem with interpretating the mechanisms behind this force drop, is that there is a great variability in the response to eccentric contractions, even though the lack of dystrophin is homogenous (Consolino and Brooks, 2004; Deconinck et al.,

1996; McArdle et al., 1991; Sacco et al., 1992) and young mdx mice (until day 15-20) show no increase in in their susceptibility to lengthening contractions (Grange et al., 2002).

A common explanation is that dystrophin is important in maintaining the integrity of the fibre, and therefore the lack of dystrophin leads to an increased fragility of the membrane (Dellorusso et al., 2001; Petrof et al., 1993), as evidenced by an increased entry of vital markers into damaged fibres. This line of thinking would be consistent with the finding that skinned fibres of dystrophic mice and control animals show no difference in their susceptibility to lengthening contractions in vitro (Lynch et al., 2000). However, studies in which the tensile strength of the dystrophic membrane was studied, showed no differences between control and mdx membranes, indicating that the intrinsic strength of the sarcolemma is unchanged (Franco and Lansman, 1990; Hutter et al., 1991).

An alternative explanation is that the rapid decrease in force seen in mdx mice after eccentric contractions is due to an altered calcium homeostasis in mdx mice caused by aberrant sarcolemmal ion channel function, particularly mechanosensitive channels, leading to an increased protection of reactive oxygen species (ROS) (Allard, 2006; Deconinck and Dan, 2007; Whitehead et al., 2006).

4.2.3 The protection is independent of hypertrophy

Previous stusdies on IGF-1 and myostatin models sggested that hypertrophy per se is beneficial in mdx mice, however when we plotted the muscle weight/ body weight, as indicator of muscle hypertrophy, against the force dropwe found that the level of protection conferred by Akt activation is not correlated with muscle hypertrophy. Indeed, systemic treatment of mdx with IGF-1 leads to a partial protection (Barton et al., 2002), even in the complete absence of hypertrophy (Schertzer et al., 2006), while blocking myostatin leads to a substantial hypertrophy without any protection (Bogdanovich et al., 2002; Bogdanovich et al., 2005). To further investigate this point we have treated our mice simultaneously with tamoxifen and rapamycin, a specific inhibitor of mTOR, the main effector of protein synthesis. Treatment with rapamycin does not inhibit the protective effect at all, clearly showing that protein synthesis through mTOR is not important for relaying this protective effect. Taking these two results, together with the findings from others, it can clearly be concluded that hypertrophy per se does not confer protection to dystrophic skeletal muscle.

4.2.4 Skinned fibres isolated from dystrophic muscles subjected to eccentric contractions *in vivo* show reduced force production, and this effect is prevented by Akt activation

To get a better understanding of the mechanism of muscle damage we have combined in-vivo eccentric contractions with in-vitro skinned fibre analysis. This analysis clearly shows that damage due to lengthening contractions is a process which occurs in vivo and leads to a decreased force production in skinned fibres. Activation of Akt for three weeks leads to a complete protection against this 'myofibrillar damage' seen control animals. An important aspect of these results is that most of skinned fibres analyzed in our studies display a force drop after eccentric contractions, indicating that the decrease in isometric force seen in control animals is not due to small subgroups of fibres which do not contract well anymore, but to a general decrease in force production from all fibres. This important and new result suggests that membrane tears are not the principal cause for the decrease in force, but that the lack of dystrophin leads to damaging downstream signals when undergoing eccentric contractions, which in their turn lead to a malfunctioning of the myofibrillar apparatus. Since it has been shown that skinned fibres from mdx and control fibres show the same susceptibility to eccentric contractions (Lynch et al., 2000), we repeated their experiments using the controlateral, non-stimulated leg. Indeed, no difference is found between dystrophic and control skeletal muscle fibres when performing in-vitro eccentric contractions therefore the

myofibrillar apparatus per se is not more fragile in mdx than in control animals. The protective effect of Akt is therefore, at least partially, due to protection at the myofibrillar level or at an upstream level in the cascade of events that lead to myofibrillar damage.

4.2.5 Akt activation does not change membrane permeability

The entry of membrane impermeable vital dyes, like Blue Evans or Procion Orange, into dystrophic muscle fibres is considered an indication of muscle damage. Indeed, various studies show an increase in dye positive fibres after eccentric contractions (Deconinck et al., 1996; Petrof et al., 1993), which is in proportion to the force drop. In our model no difference could be detected between either stimulated or not stimulated mdx muscles, for both treated as well as control animals. This discrepancy can be explained by the intensity of exercise to which the muscles are subjected. When stretching a muscle excessively, outside of either physiological ranges or environments, interpretation can become more difficult. In our model we used eccentric lengthening of the gastrocnemius by moving the foot clearly over a physiological range. This very likely is insufficient to induce a clear accumulation of dye inside a significant amount of fibres. Indeed, the reason why some studies do not find any difference in force drop (McArdle et al., 1991; Sacco et al., 1992) is most likely explained by the fact that they performed excessive stimulation/stretching protocols. All studies in which an increase in dye-positive fibres is seen after eccentric contractions, show a much bigger decrease in force drop than the increase in dye-positive fibres (Deconinck et al., 1996; Petrof et al., 1993). This can be explained by the fact that for large proteins such as creatine kinase and albumine, to leave or enter the cell large membrane defects need to be present (McNeil and Khakee, 1992). According to our data, the primary reason for the force drop is due to myofibrillar dysfunction, which can be explained by an increased calcium entry leading to increased calpain mediated myofibrillar protein degradation (Goll et al., 2003; Zaidi and Narahara, 1989) or to increased reactive oxygen species generation (Rando et al., 1998). In this case, sarcolemmal defects would be nothing else than a secondary effect, in some cases leading to necrosis, clearly explaining why the number of dye-positive fibres is always substantially lower than the force drop.
A Ca^{2+}-permeable leak channel which is active in resting muscle and has a higher open probability in *mdx* muscle has been described by several groups (Fong et al., 1990; Franco and Lansman, 1990). It has been demonstrated that this channel can be activated or inactivated by stretch and in dystrophic muscles these channels might act as a source of additional Ca^{2+} entry (Franco-Obregon and Lansman, 2002; Whitehead et al., 2006; Yeung et al., 2005).

4.2.6 Akt activation does not lead to dystrophin re-expression

Recently it has been suggested that treatment of mdx mice with proteasome inhibitors can rescue a truncated form of dystrophin from degradation. This mini-dystrophin would be still functional, despite missing part of its C-terminus, since it shows a correct cellular localization together with the other components of the dystrophin-glycoprotein complex (Assereto et al., 2006; Bonuccelli et al., 2007; Bonuccelli et al., 2003). However, we found that staining with a polyclonal antibody, which specifically stains the N-terminal part of the protein, shows no differences between treated and control animals. Occasional revertent fibres are present in both groups, but the blocking of the proteasome by Akt is not sufficient to avoid degradation of the truncated dystrophin protein.

4.2.7 Akt activation leads to an increased utrophin and desmin content

An important finding in our study is that activation of Akt leads to an increase in utrophin and desmin content. Utrophin over-expression from birth in mdx mice is known to prevent dystrophy completely (Tinsley et al., 1998), while up-regulation later in life shows more limited, dose-dependent effects (Squire et al., 2002). Various experimental models have shown beneficial effects in dystrophic muscle due to up-regulation of utrophin (Krag et al., 2004; Nguyen et al., 2002; Stupka et al., 2006), yet inducible over-expression of utrophin in 30 days old mdx mice is not sufficient to lead to amelioration of the dystrophic phenotype (Squire et al., 2002). Transfection of mature dystrophic muscles with an adenovirus containing an utrophin transgene on the other hand leads to an increased protection against lengthening contractions (Ebihara et al., 2000). These findings suggest that a partial explanation of the protective effect of Akt in dystrophic muscles, is the increased utrophin content. It is not clear as to why discrepancies exist in the degree of protection conferred by utrophin upregulation, but it is tempting to think that differences are created by the model used for eccentric contractions. It has been suggested that a threshold for utrophin expression exist below which pathology deteriorates (Deconinck et al., 1997). This threshold is obviously dependent of the system used for studying various pathological symptoms. In our model of eccentric contractions, which can be considered mild, a protective effect can be seen because stretching is not exceeding certain physiological limits.

It remains speculation as to how utrophin can protect against damage occurring at the myofibrillar level. One hypothesis is that an increase in utrophin leads to an improved calcium handling in conditions of stress (Deconinck et al., 1997). It is well known that mitochondrial calcium overload in turn, can lead to an increased ROS production (Brookes et al., 2004). As stated previously, after eccentric contraction intracellular calcium in dystrophic fibres increases (Yeung et al., 2005), making it tempting to assume that this initiates a cascade leading to activation of ROS, either through mitochondrial overload or increased NADPH-oxidase activity (Grote et al., 2003; Javesghani et al., 2002).

Another factor which could explain an increased resistance to mechanical stretch, is the increased rigidity of the cytoskeleton. It is possible that the increase in desmin content contributes to the reduced swelling of skinned fibres. Desmin is known to provide rigidity to the Z-disk by forming a three-dimensional scaffold around it. This up-regulation is of particular interest since it is known that eccentric exercise in healthy individuals, if repeated, leads to cytoskeletal adaptations, in particular desmin up-regulation (Woolstenhulme et al., 2006). It has been proposed that this cytoskeletal respons is responsible for the protective effect from damage when repeating eccentric contractions (McHugh, 2003). In contrast with this line of thinking is the finding that knock-out mice for desmin show the same force drop after eccentric contractions as their wild-type controls even though a high frequency fatigue protocol shows an increased sensitivity to aberrant EC-coupling (Wieneke et al., 2000). An increased protection of the t-tubules through an increased desmin-concentration would fit nicely into the picture that Ca-handling is improved in mdx mice after Akt activation avoiding damage due to calcium overload.

Summarizing all these results, it is clear that Akt leads to protection against eccentric contractions, which prevents myofibrillar damage. This protection is possibly due to an increased utrophin content together with an upregulation of desmin, leading to an improved calcium homeostasis after eccentric contractions.

Bibliography

Abmayr, S., Gregorevic, P., Allen, J. M., and Chamberlain, J. S. (2005). Phenotypic improvement of dystrophic muscles by rAAV/microdystrophin vectors is augmented by Igf1 codelivery. Mol Ther *12*, 441-450.

Allard, B. (2006). Sarcolemmal ion channels in dystrophin-deficient skeletal muscle fibres. J Muscle Res Cell Motil *27*, 367-373.

Amthor, H., Macharia, R., Navarrete, R., Schuelke, M., Brown, S. C., Otto, A., Voit, T., Muntoni, F., Vrbova, G., Partridge, T., *et al.* (2007). Lack of myostatin results in excessive muscle growth but impaired force generation. Proc Natl Acad Sci U S A *104*, 1835-1840.

Assereto, S., Stringara, S., Sotgia, F., Bonuccelli, G., Broccolini, A., Pedemonte, M., Traverso, M., Biancheri, R., Zara, F., Bruno, C., *et al.* (2006). Pharmacological rescue of the dystrophin-glycoprotein complex in Duchenne and Becker skeletal muscle explants by proteasome inhibitor treatment. Am J Physiol Cell Physiol *290*, C577-582.

Barton, E. R., Morris, L., Musaro, A., Rosenthal, N., and Sweeney, H. L. (2002). Muscle-specific expression of insulin-like growth factor I counters muscle decline in mdx mice. J Cell Biol *157*, 137-148.

Bezakova, G., and Lomo, T. (2001). Muscle activity and muscle agrin regulate the organization of cytoskeletal proteins and attached acetylcholine receptor (AchR) aggregates in skeletal muscle fibers. J Cell Biol *153*, 1453-1463.

Blough, E. R., Rennie, E. R., Zhang, F., and Reiser, P. J. (1996). Enhanced electrophoretic separation and resolution of myosin heavy chains in mammalian and avian skeletal muscles. Anal Biochem *233*, 31-35.

Bogdanovich, S., Krag, T. O., Barton, E. R., Morris, L. D., Whittemore, L. A., Ahima, R. S., and Khurana, T. S. (2002). Functional improvement of dystrophic muscle by myostatin blockade. Nature *420*, 418-421.

Bogdanovich, S., Perkins, K. J., Krag, T. O., Whittemore, L. A., and Khurana, T. S. (2005). Myostatin propeptide-mediated amelioration of dystrophic pathophysiology. Faseb J *19*, 543-549.

Bonuccelli, G., Sotgia, F., Capozza, F., Gazzerro, E., Minetti, C., and Lisanti, M. P. (2007). Localized treatment with a novel FDA-approved proteasome inhibitor blocks the degradation of dystrophin and dystrophin-associated proteins in mdx mice. Cell Cycle *6*, 1242-1248.

Bonuccelli, G., Sotgia, F., Schubert, W., Park, D. S., Frank, P. G., Woodman, S. E., Insabato, L., Cammer, M., Minetti, C., and Lisanti, M. P. (2003). Proteasome inhibitor (MG-132) treatment of mdx mice rescues the expression and membrane localization of dystrophin and dystrophin-associated proteins. Am J Pathol *163*, 1663-1675.

Bothe, G. W., Haspel, J. A., Smith, C. L., Wiener, H. H., and Burden, S. J. (2000). Selective expression of Cre recombinase in skeletal muscle fibers. Genesis *26*, 165-166.

Bottinelli, R., Canepari, M., Pellegrino, M. A., and Reggiani, C. (1996). Force-velocity properties of human skeletal muscle fibres: myosin heavy chain isoform and temperature dependence. JPhysiol *495*, 573-586.

Brookes, P. S., Yoon, Y., Robotham, J. L., Anders, M. W., and Sheu, S. S. (2004). Calcium, ATP, and ROS: a mitochondrial love-hate triangle. Am J Physiol Cell Physiol *287*, C817-833.

Bruusgaard, J. C., Brack, A. S., Hughes, S. M., and Gundersen, K. (2005). Muscle hypertrophy induced by the Ski protein: cyto-architecture and ultrastructure. Acta Physiol Scand *185*, 141-149.

Consolino, C. M., and Brooks, S. V. (2004). Susceptibility to sarcomere injury induced by single stretches of maximally activated muscles of mdx mice. J Appl Physiol *96*, 633-638.

D'Antona, G., Lanfranconi, F., Pellegrino, M. A., Brocca, L., Adami, R., Rossi, R., Moro, G., Miotti, D., Canepari, M., and Bottinelli, R. (2006). Skeletal muscle hypertrophy and structure and function of skeletal muscle fibres in male body builders. J Physiol *570*, 611-627.

Deconinck, N., and Dan, B. (2007). Pathophysiology of duchenne muscular dystrophy: current hypotheses. Pediatr Neurol *36*, 1-7.

Deconinck, N., Ragot, T., Marechal, G., Perricaudet, M., and Gillis, J. M. (1996). Functional protection of dystrophic mouse (mdx) muscles after adenovirus-mediated transfer of a dystrophin minigene. Proc Natl Acad Sci U S A *93*, 3570-3574.

Deconinck, N., Tinsley, J., De Backer, F., Fisher, R., Kahn, D., Phelps, S., Davies, K., and Gillis, J. M. (1997). Expression of truncated utrophin leads to major functional improvements in dystrophin-deficient muscles of mice. Nat Med *3*, 1216-1221.

Dellorusso, C., Crawford, R. W., Chamberlain, J. S., and Brooks, S. V. (2001). Tibialis anterior muscles in mdx mice are highly susceptible to contraction-induced injury. J Muscle Res Cell Motil *22*, 467-475.

Ebihara, S., Guibinga, G. H., Gilbert, R., Nalbantoglu, J., Massie, B., Karpati, G., and Petrof, B. J. (2000). Differential effects of dystrophin and utrophin gene transfer in immunocompetent muscular dystrophy (mdx) mice. Physiol Genomics *3*, 133-144.

Esmarck, B., Andersen, J. L., Olsen, S., Richter, E. A., Mizuno, M., and Kjaer, M. (2001). Timing of postexercise protein intake is important for muscle hypertrophy with resistance training in elderly humans. J Physiol *535*, 301-311.

Fong, P. Y., Turner, P. R., Denetclaw, W. F., and Steinhardt, R. A. (1990). Increased activity of calcium leak channels in myotubes of Duchenne human and mdx mouse origin. Science *250*, 673-676.

Franco, A., Jr., and Lansman, J. B. (1990). Calcium entry through stretch-inactivated ion channels in mdx myotubes. Nature *344*, 670-673.

Franco-Obregon, A., and Lansman, J. B. (2002). Changes in mechanosensitive channel gating following mechanical stimulation in skeletal muscle myotubes from the mdx mouse. J Physiol *539*, 391-407.

Goll, D. E., Thompson, V. F., Li, H., Wei, W., and Cong, J. (2003). The calpain system. Physiol Rev *83*, 731-801.

Grange, R. W., Gainer, T. G., Marschner, K. M., Talmadge, R. J., and Stull, J. T. (2002). Fast-twitch skeletal muscles of dystrophic mouse pups are resistant to injury from acute mechanical stress. Am J Physiol Cell Physiol *283*, C1090-1101.

Grote, K., Flach, I., Luchtefeld, M., Akin, E., Holland, S. M., Drexler, H., and Schieffer, B. (2003). Mechanical stretch enhances mRNA expression and proenzyme release of matrix metalloproteinase-2 (MMP-2) via NAD(P)H oxidase-derived reactive oxygen species. Circ Res *92*, e80-86.

Hutter, O. F., Burton, F. L., and Bovell, D. L. (1991). Mechanical properties of normal and mdx mouse sarcolemma: bearing on function of dystrophin. J Muscle Res Cell Motil *12*, 585-589.

Javesghani, D., Magder, S. A., Barreiro, E., Quinn, M. T., and Hussain, S. N. (2002). Molecular characterization of a superoxide-generating NAD(P)H oxidase in the ventilatory muscles. Am J Respir Crit Care Med *165*, 412-418.

Kim, Y. K., Kim, S. J., Yatani, A., Huang, Y., Castelli, G., Vatner, D. E., Liu, J., Zhang, Q., Diaz, G., Zieba, R., *et al.* (2003). Mechanism of enhanced cardiac function in mice with hypertrophy induced by overexpressed Akt. J Biol Chem *278*, 47622-47628.

Krag, T. O., Bogdanovich, S., Jensen, C. J., Fischer, M. D., Hansen-Schwartz, J., Javazon, E. H., Flake, A. W., Edvinsson, L., and Khurana, T. S. (2004). Heregulin ameliorates the dystrophic phenotype in mdx mice. Proc Natl Acad Sci U S A *101*, 13856-13860.

Kroll, J., Cobo, P., and Sato, T. N. (2003). Versatile inducible activation system of Akt/PKB signaling pathway in mice. Genesis *35*, 160-163.

Lai, K. M., Gonzalez, M., Poueymirou, W. T., Kline, W. O., Na, E., Zlotchenko, E., Stitt, T. N., Economides, A. N., Yancopoulos, G. D., and Glass, D. J. (2004). Conditional activation of akt in adult skeletal muscle induces rapid hypertrophy. Mol Cell Biol *24*, 9295-9304.

Leblond, H., L'Esperance, M., Orsal, D., and Rossignol, S. (2003). Treadmill locomotion in the intact and spinal mouse. J Neurosci *23*, 11411-11419.

Lynch, G. S., Rafael, J. A., Chamberlain, J. S., and Faulkner, J. A. (2000). Contraction-induced injury to single permeabilized muscle fibers from mdx, transgenic mdx, and control mice. Am J Physiol Cell Physiol *279*, C1290-1294.

Mammucari, C., Milan, G., Romanello, V., Masiero, E., Rudolf, R., Del Piccolo, P., Burden, S. J., Di Lisi, R., Sandri, C., Zhao, J., *et al.* (2007). FoxO3 Controls Autophagy in Skeletal Muscle In Vivo. Cell Metab *6*, 458-471.

McArdle, A., Edwards, R. H., and Jackson, M. J. (1991). Effects of contractile activity on muscle damage in the dystrophin-deficient mdx mouse. Clin Sci (Lond) *80*, 367-371.

McHugh, M. P. (2003). Recent advances in the understanding of the repeated bout effect: the protective effect against muscle damage from a single bout of eccentric exercise. Scand J Med Sci Sports *13*, 88-97.

McNeil, P. L., and Khakee, R. (1992). Disruptions of muscle fiber plasma membranes. Role in exercise-induced damage. Am J Pathol *140*, 1097-1109.

Midrio, M. (2006). The denervated muscle: facts and hypotheses. A historical review. Eur J Appl Physiol *98*, 1-21.

Musaro, A., McCullagh, K., Paul, A., Houghton, L., Dobrowolny, G., Molinaro, M., Barton, E. R., Sweeney, H. L., and Rosenthal, N. (2001). Localized Igf-1 transgene expression sustains hypertrophy and regeneration in senescent skeletal muscle. Nat Genet *27*, 195-200.

Nguyen, H. H., Jayasinha, V., Xia, B., Hoyte, K., and Martin, P. T. (2002). Overexpression of the cytotoxic T cell GalNAc transferase in skeletal muscle inhibits muscular dystrophy in mdx mice. Proc Natl Acad Sci U S A *99*, 5616-5621.

Pallafacchina, G., Calabria, E., Serrano, A. L., Kalhovde, J. M., and Schiaffino, S. (2002). A protein kinase B-dependent and rapamycin-sensitive pathway controls skeletal muscle growth but not fiber type specification. Proc Natl Acad Sci U S A *99*, 9213-9218.

Peter, A. K., and Crosbie, R. H. (2006). Hypertrophic response of Duchenne and limb-girdle muscular dystrophies is associated with activation of Akt pathway. Exp Cell Res *312*, 2580-2591.

Petrof, B. J., Shrager, J. B., Stedman, H. H., Kelly, A. M., and Sweeney, H. L. (1993). Dystrophin protects the sarcolemma from stresses developed during muscle contraction. Proc Natl Acad Sci U S A *90*, 3710-3714.

Rando, T. A., Disatnik, M. H., Yu, Y., and Franco, A. (1998). Muscle cells from mdx mice have an increased susceptibility to oxidative stress. Neuromuscul Disord *8*, 14-21.

Reggiani, C., Potma, E. J., Bottinelli, R., Canepari, M., Pellegrino, M. A., and Stienen, G. J. (1997). Chemo-mechanical energy transduction in relation to myosin isoform composition in skeletal muscle fibres of the rat. J Physiol *502 (Pt 2)*, 449-460.

Rota, M., Boni, A., Urbanek, K., Padin-Iruegas, M. E., Kajstura, T. J., Fiore, G., Kubo, H., Sonnenblick, E. H., Musso, E., Houser, S. R., *et al.* (2005). Nuclear targeting of Akt enhances ventricular function and myocyte contractility. Circ Res *97*, 1332-1341.

Roy, R. R., Monke, S. R., Allen, D. L., and Edgerton, V. R. (1999). Modulation of myonuclear number in functionally overloaded and exercised rat plantaris fibers. J Appl Physiol *87*, 634-642.

Sacco, P., Jones, D. A., Dick, J. R., and Vrbova, G. (1992). Contractile properties and susceptibility to exercise-induced damage of normal and mdx mouse tibialis anterior muscle. Clin Sci (Lond) *82*, 227-236.

Sacheck, J. M., Hyatt, J. P., Raffaello, A., Jagoe, R. T., Roy, R. R., Edgerton, V. R., Lecker, S. H., and Goldberg, A. L. (2007). Rapid disuse and denervation atrophy involve transcriptional changes similar to those of muscle wasting during systemic diseases. Faseb J *21*, 140-155.

Sakamoto, K., Hirshman, M. F., Aschenbach, W. G., and Goodyear, L. J. (2002). Contraction regulation of Akt in rat skeletal muscle. J Biol Chem *277*, 11910-11917.

Sandri, M., Sandri, C., Gilbert, A., Skurk, C., Calabria, E., Picard, A., Walsh, K., Schiaffino, S., Lecker, S. H., and Goldberg, A. L. (2004). Foxo transcription factors induce the atrophy-related ubiquitin ligase atrogin-1 and cause skeletal muscle atrophy. Cell *117*, 399-412.

Schertzer, J. D., Ryall, J. G., and Lynch, G. S. (2006). Systemic administration of IGF-I enhances oxidative status and reduces contraction-induced injury in skeletal muscles of mdx dystrophic mice. Am J Physiol Endocrinol Metab *291*, E499-505.

Schertzer, J. D., van der Poel, C., Shavlakadze, T., Grounds, M. D., and Lynch, G. S. (2007). Muscle specific overexpression of IGF-I improves E-C coupling in skeletal muscle fibers from dystrophic mdx mice. Am J Physiol Cell Physiol.

Schiekofer, S., Shiojima, I., Sato, K., Galasso, G., Oshima, Y., and Walsh, K. (2006). Microarray analysis of Akt1 activation in transgenic mouse hearts reveals transcript expression profiles associated with compensatory hypertrophy and failure. Physiol Genomics *27*, 156-170.

Squire, S., Raymackers, J. M., Vandebrouck, C., Potter, A., Tinsley, J., Fisher, R., Gillis, J. M., and Davies, K. E. (2002). Prevention of pathology in mdx mice by expression of utrophin: analysis using an inducible transgenic expression system. Hum Mol Genet *11*, 3333-3344.

Stitt, T. N., Drujan, D., Clarke, B. A., Panaro, F., Timofeyva, Y., Kline, W. O., Gonzalez, M., Yancopoulos, G. D., and Glass, D. J. (2004). The IGF-1/PI3K/Akt pathway prevents expression of muscle atrophy-induced ubiquitin ligases by inhibiting FOXO transcription factors. Mol Cell *14*, 395-403.

Stupka, N., Plant, D. R., Schertzer, J. D., Emerson, T. M., Bassel-Duby, R., Olson, E. N., and Lynch, G. S. (2006). Activated calcineurin ameliorates contraction-induced injury to skeletal muscles of mdx dystrophic mice. J Physiol *575*, 645-656.

Tinsley, J., Deconinck, N., Fisher, R., Kahn, D., Phelps, S., Gillis, J. M., and Davies, K. (1998). Expression of full-length utrophin prevents muscular dystrophy in mdx mice. Nat Med *4*, 1441-1444.

Whitehead, N. P., Yeung, E. W., and Allen, D. G. (2006). Muscle damage in mdx (dystrophic) mice: role of calcium and reactive oxygen species. Clin Exp Pharmacol Physiol *33*, 657-662.

Wieneke, S., Stehle, R., Li, Z., and Jockusch, H. (2000). Generation of tension by skinned fibers and intact skeletal muscles from desmin-deficient mice. Biochem Biophys Res Commun *278*, 419-425.

Woolstenhulme, M. T., Conlee, R. K., Drummond, M. J., Stites, A. W., and Parcell, A. C. (2006). Temporal response of desmin and dystrophin proteins to progressive resistance exercise in human skeletal muscle. J Appl Physiol *100*, 1876-1882.

Yeung, E. W., Whitehead, N. P., Suchyna, T. M., Gottlieb, P. A., Sachs, F., and Allen, D. G. (2005). Effects of stretch-activated channel blockers on [Ca2+]i and muscle damage in the mdx mouse. J Physiol *562*, 367-380.

Zaidi, S. I., and Narahara, H. T. (1989). Degradation of skeletal muscle plasma membrane proteins by calpain. J Membr Biol *110*, 209-216.